electronics

MDPI

Article

Multi-Strategy Improved Particle Swarm Optimization Algorithm and Gazelle Optimization Algorithm and Application

Santuan Qin, Huadie Zeng, Wei Sun, Jin Wu and Junhua Yang *

School of Electronic Engineering, Xi'an University of Posts and Telecommunications, Xi'an 710121, China; qinsantuan@xupt.edu.cn (S.Q.); zenghuadie@stu.xupt.edu.cn (H.Z.); sw@stu.xupt.edu.cn (W.S.); lifewujin@xupt.edu.cn (J.W.)
* Correspondence: yjh@xupt.edu.cn

Abstract: In addressing the challenges associated with low convergence accuracy and unstable optimization results in the original gazelle optimization algorithm (GOA), this paper proposes a novel approach incorporating chaos mapping termed multi-strategy particle swarm optimization with gazelle optimization algorithm (MPSOGOA). In the population initialization stage, segmented mapping is integrated to generate a uniformly distributed high-quality population which enhances diversity, and global perturbation of the population is added to improve the convergence speed in the early iteration and the convergence accuracy in the late iteration. By combining particle swarm optimization (PSO) and GOA, the algorithm leverages individual experiences of gazelles, which improves convergence accuracy and stability. Tested on 35 benchmark functions, MPSOGOA demonstrates superior performance in convergence accuracy and stability through Friedman tests and Wilcoxon signed-rank tests, surpassing other metaheuristic algorithms. Applied to engineering optimization problems, including constrained implementations, MPSOGOA exhibits excellent optimization performance.

Keywords: gazelle optimization algorithm; optimization methods; particle swarm optimization; Wilcoxon rank sum test

check for updates

Citation: Qin, S.; Zeng, H.; Sun, W.; Wu, J.; Yang, J. Multi-Strategy Improved Particle Swarm Optimization Algorithm and Gazelle Optimization Algorithm and Application. *Electronics* **2024**, *13*, 1580. https://doi.org/10.3390/electronics13081580

Academic Editor: Maciej Ławryńczuk

Received: 13 March 2024
Revised: 10 April 2024
Accepted: 17 April 2024
Published: 20 April 2024

Copyright: © 2024 by the authors. Licensee MDPI, Basel, Switzerland. This article is an open access article distributed under the terms and conditions of the Creative Commons Attribution (CC BY) license (https://creativecommons.org/licenses/by/4.0/).

1. Introduction

Optimization is the process wherein individuals, under certain constraints, employ specific methods and techniques to enhance the performance of existing entities, thereby seeking the optimal solution to a given problem within the solution space. Nowadays, optimization issues are ubiquitous in daily life and engineering technology, serving as popular research topics in fields such as automation, computer science, telecommunications, aerospace, and more.

Heuristic algorithms, which draw inspiration from natural laws, can be broadly classified into the following categories: physical methods based on principles such as gravity, temperature, and inertia, which randomly search for the optimal solution to optimization problems, for instance, methods like gravitational search [1]; simulated annealing [2]; and black hole algorithms [3]. Evolutionary algorithms, grounded in Darwin's theory, facilitate the gradual discovery of optimal solutions as the individuals within a population evolve through iterations during the search process. Typical examples include genetic algorithms [4], biogeography-based optimization algorithms [5], artificial algae algorithm [6], widow optimization search algorithm [7], and taboo search algorithm [8]. In a population of organisms, each individual has its own role, and communication among individuals enables the acquisition of superior information, ultimately completing the population's evolution. Swarm intelligence optimization algorithms are essentially mathematical models created by researchers to simulate the behavior of collective animals in the natural world.

Inspired by various behaviors exhibited by natural biological populations such as insects, birds, fish, and herds, numerous swarm intelligence optimization algorithms have been proposed and have played a crucial role in many scientific and engineering applications. Mayer Martin Janos et al. used genetic algorithms to find an optimal solution for a hybrid renewable energy system at the home level that is both economical and environmentally friendly [9]. Laith Abualigah and Muhammad Alkhrabsheh can effectively solve the problem of cloud computing task scheduling using a hybrid multilateral optimizer optimized by a genetic algorithm [10]. G Lodewijks et al. [11] significantly reduced CO2 emissions in the airport baggage handling transportation system by applying particle swarm optimization (PSO) algorithm. Bilal Hussain [12] proposed decomposition weighting and PSO (DWS-PSO), which provides a new solution for price-driven demand response and home energy management systems for renewable energy and storage scheduling. Paul Kaushik and Hati Debolina [13] applied the Harris hawk optimization algorithm to household energy management, resulting in reduced power consumption. Jiang [14] and others utilized the artificial bee colony algorithm for ship structural profile optimization. Abd Elaziz Mohamed and colleagues [15] improved the artificial rabbit optimization algorithm for skin cancer prediction, achieving reliable predictive results. Bishla Sandeep and team [16] employed the chimpanzee optimization algorithm for optimizing the scheduling of batteries in electric vehicles. Percin Hasan Bektas and Caliskan Abuzer [17] utilized the whale optimization algorithm to control fuel cell systems. Jagadish Kumar N. and Balasubramanian C. [18] implemented the widow optimization algorithm for cloud service resource scheduling, effectively reducing the cost of cloud services. Zeng [19] optimized heterogeneous wireless sensor network coverage using the wild horse optimization algorithm, achieving significant coverage and connectivity. Chhabra Amit [20] and others applied the vulture search optimization algorithm in feature selection. Liu and team [21] predicted the lifespan of lithium-ion batteries using an improved sparrow algorithm. Xu and colleagues [22] performed feature selection using the binary arithmetic optimization algorithm.

With the development of heuristic algorithms, integrating different optimization mechanisms and evolutionary characteristics into algorithms, as well as drawing on each other's strengths and overcoming the inherent deficiencies of the algorithms, has gradually become a new trend in the development of optimization algorithms. Chen [23] and others combined the differential evolution algorithm with the biogeography-based optimization algorithm for application in the three-dimensional bin packing problem, significantly improving the utilization of box volume. Long and colleagues [24] integrated the bacterial foraging optimization algorithm and simulated annealing algorithm in local path planning for unmanned vessels, efficiently planning obstacle avoidance paths. Zou and team [25] employed a cross-strategy of whale optimization algorithm and genetic algorithm in the cogeneration system, reducing energy consumption. Ramachandran Murugan [26] and others balanced the locust optimization algorithm and the Harris hawk optimization algorithm in the initial and later convergence stages, applying it to the economic dispatch problem of the thermal-electric field. Manar Hamza and team [27] combined the differential evolution algorithm with the arithmetic optimization algorithm, enhancing the optimization effect. Pashaei Elham and Pashaei Elnaz [28] combined the binary arithmetic optimization algorithm with the simulated annealing algorithm, improving computational accuracy. Bhowmik Sandeep and Acharyya Sriyankar [29] combined the differential evolution algorithm with the genetic algorithm in the image encryption problem.

PSO, as one of the classic metaheuristic algorithms, has been applied in many fields in recent years. Valiollah Panahizadeh [30] used PSO to improve the impact strength and elastic modulus of polyamide-based nanocomposites. Kim Kang Hyun et al. [31] used the PSO algorithm to optimize the drainage system of the undersea tunnel, significantly reducing the construction cost. Kirti Pal et al. [32] optimized the installation cost of flexible AC transmission system through PSO to improve the stability and load conditions of the power system. Zezhong Kang et al. [33] applied the improved PSO algorithm to the rural power grid auxiliary cogeneration system in the North China Plain to determine the optimal unit capacity configuration. In addition, particle swarm computing is often combined with other methods to improve the search performance and has been applied in various fields. Somporn Sirisumrannukul et al. [34] combined artificial neural networks (ANNs) and PSO algorithms to not only collect real-time environmental data and air conditioner usage records, but also autonomously adjust the operation of air conditioners. Sathasivam Karthikeyan et al. [35] adopted the artificial bee swarm (ABC) algorithm and PSO algorithm to optimize the Boost converter and improve the efficiency of the system. Norouzi Hadi and Bazargan Jalal [36] used the linear Musjingen method and PSO algorithm for the first time to study river water pollution and calculate the time change of pollution concentration at different river locations. Shaikh Muhammad Suhail [37] and others combined the PSO algorithm with the moth-flame optimization algorithm for application in power transmission systems. Makhija Divya and colleagues [38] overcame the drawbacks of both the local search of the PSO algorithm and the global search of the grey wolf optimization algorithm, applying this method to the workflow task scheduling problem. Tijani Muhammed Adekilekun and team [39] combined the PSO algorithm with the bat algorithm to effectively avoid falling into local optima, applying this method to the joint economic dispatch scheduling problem in power systems. Osei Kwakye Jeremiah [40] and others combined the PSO algorithm with the gravitational search algorithm to overcome premature convergence. Wang and colleagues [41] integrated the PSO algorithm with the marine predator algorithm. Samantaray Sandeep and team [42] combined the PSO algorithm with the slime mold algorithm in flood flow prediction. Wang [43] and others combined the PSO algorithm with the artificial bee colony algorithm in underwater terrain-assisted navigation, enhancing the matching effect.

Among the swarm intelligence optimization algorithms mentioned above, the gazelle optimization algorithm (GOA) [44] has gained increasing usage in practical engineering optimization problems due to its advantage in finding the optimal solution in test functions. However, due to its inherent drawbacks such as low convergence accuracy and unstable optimization results, it may not yield satisfactory results in all optimization problems. This paper aims to improve the shortcomings of the GOA, addressing its deficiencies and enhancing the convergence speed and stability of GOA. The main contributions of this work are as follows:

1. Initializing the population through chaotic mapping to improve the quality and diversity of initial solutions.
2. Implementing phased population perturbation to enhance the stability of optimization results while maintaining high precision.
3. Combined with PSO, the role of the individual experience of the gazelle in the escape process is used to improve the ability of the algorithm to jump out of the local optimum.

This paper is divided into seven sections. Section 2 provides a review and analysis of the literature. Section 3 briefly describes the principles of the traditional GOA. Section 4 introduces the MPSOGOA. Section 5 presents the experimental design for testing functions and engineering applications. Section 6 discusses the experimental results. The conclusion is presented in the final section.

2. Gazelle Optimization Algorithm

2.1. Exploration Phase

During this phase, the gazelles, without predators or any signs of their presence, remain in a calm state, grazing. Drawing on the foraging behavior of gazelles freely grazing, the algorithm simulates the random movements of gazelles within the solution space. In nature, the strongest gazelles not only possess strong survival abilities but also lead other gazelles in evading predators, with the fittest individual in the population being referred to as the alpha gazelle. Assuming the d-dimensional alpha gazelle is represented as shown:

$$x' = [x'(1)\ x'(2)\ \cdots\ x'(d-1)\ x'(d)] \tag{1}$$

We extend the top gazelle individuals to construct an $n \times d$ dimensional Elite matrix, where n represents the population number and d represents the dimension. The matrix is given by Equation (2):

$$\text{Elite} = \begin{bmatrix} x'_{1,1}(1) & x'_{1,2}(2) & \cdots & x'_{1,d-1}(d-1) & x'_{1,d}(d) \\ x'_{2,1}(1) & x'_{2,2}(2) & \cdots & x'_{2,d-1}(d-1) & x'_{2,d}(d) \\ \vdots & \vdots & x'_{i,j} & \vdots & \vdots \\ x'_{n,1}(1) & x'_{n,2}(2) & \cdots & x'_{n,d-1}(d-1) & x'_{n,d}(d) \end{bmatrix} \tag{2}$$

The updating strategy of individual positions in the gazelle population is related to the current optimal individual position. Based on the distance between the current optimal individual and its own grazing position, the individual position is updated, with the displacement step controlled by Brownian motion. The mathematical model is shown in:

$$\text{gazelle}_{t+1} = \text{gazelle}_t + s \cdot R \cdot R_B \cdot (\text{Elite}_t - R_B \cdot \text{gazelle}_t) \tag{3}$$

where gazelle_{t+1} and gazelle_t represent the positions at the (t + 1)th and t-th iterations, respectively. s denotes the speed of gazelle movement during free grazing, R is a random number between 0 and 1, Elite represents the matrix of the alpha gazelle, and $\mathrm{R_B}$ is the vector of Brownian motion, as given by Equations (4) and (5):

$$f(x;\mu;\sigma) = \frac{1}{\sqrt{2\pi\sigma^2}} \exp\left(-\frac{(x-\mu)^2}{2\sigma^2}\right) = \frac{1}{\sqrt{2\pi}} \exp\left(-\frac{x^2}{2}\right) \tag{4}$$

where μ and σ are constants, μ = 0 is the mean value, and σ^2 = 1 is the unit variance.

$$\mathrm{R}_B = \begin{bmatrix} f_{1,1} & f_{1,2} & \cdots & f_{1,d-1} & f_{1,d} \\ f_{2,1} & f_{2,2} & \cdots & f_{2,d-1} & f_{2,d} \\ \vdots & \vdots & f_{i,j} & \vdots & \vdots \\ f_{n,1} & f_{n,2} & \cdots & f_{n,d-1} & f_{n,d} \end{bmatrix} \tag{5}$$

2.2. Exploitation Phase

In this phase, the algorithm simulates the fleeing behavior of gazelles upon detecting predators, with each phase adopting movements in opposite directions based on the parity of the iteration count. Equation (6) for Levy flight motion is provided in [39]:

$$f'(\alpha) = \frac{0.05x}{|y|^{\frac{1}{\alpha}}} \tag{6}$$

where α = 1.5, $x = Normal(0, \sigma_x^2)$, $y = Normal(0, \sigma_y^2)$, $\sigma_y = 1$, σ_x is given by:

$$\sigma_x = \left[\frac{\Gamma(1+\alpha)\sin\left(\frac{\pi\alpha}{2}\right)}{\Gamma\left(\frac{(1+\alpha)}{2}\right)\alpha 2^{\frac{(\alpha-1)}{2}}}\right]^{\frac{1}{\alpha}} \tag{7}$$

Upon spotting a predator, gazelles immediately initiate escape, simulating the gazelle's fleeing behavior using a Lévy flight. The escape model is provided by:

$$gazelle_{t+1} = gazelle_t + S \cdot \mu \cdot R \cdot R_L \cdot (Elite_t - R_L \cdot gazelle_t) \tag{8}$$

where S represents the maximum speed achievable by the gazelle during the escape process, and R_L is a vector of random numbers based on the Lévy flight, as given by:

$$R_L = \begin{bmatrix} f'_{1,1} & f'_{1,2} & \cdots & f'_{1,d-1} & f'_{1,d} \\ f'_{2,1} & f'_{2,2} & \cdots & f'_{2,d-1} & f'_{1,d} \\ \vdots & \vdots & x'_{i,j} & \vdots & \vdots \\ f'_{n,1} & f'_{n,2} & \cdots & f'_{n,d-1} & f'_{n,d} \end{bmatrix} \tag{9}$$

While tracking gazelles, predators move in the same direction. Therefore, during the gazelle's escape process, the predators also exhibit exploratory behavior in the search space. However, predators are slower in the initial phase of the pursuit, and a Brownian motion is used to simulate the chasing process, followed by the adoption of a Lévy flight in the later stages to model the predator's behavior. The mathematical model for the predator's pursuit of gazelles is provided by:

$$gazelle_{t+1} = gazelle_t + S \cdot \mu \cdot CF \cdot R_B \cdot (Elite_t - R_L \cdot gazelle_t) \tag{10}$$

where CF represents the cumulative effect of predators, as shown in:

$$CF = \left(1 - \frac{t}{T}\right)^{\frac{2t}{T}} \tag{11}$$

The survival rate of gazelles in the face of predators is 0.66, which implies that predators have a 34% chance of successful hunting. Using predator success rates (PSRs) to represent the success rate of predators, a mathematical model of the gazelle escape process is established, as shown in:

$$gazelle_{t+1} = \begin{cases} gazelle_t + CF[LB + R \cdot (UB - LB)] \cdot U & if \text{ r} \leq \text{PSRs} \\ gazelle_t + [PSRs \cdot (1 - r) + r] \cdot (gazelle_{r1} - gazelle_{r2}) \text{ else} \end{cases} \tag{12}$$

where r_1 and r_2 are random indices of the gazelle population. U is a binary matrix representing the logical value obtained by comparing random numbers in the range of [0, 1] with 0.34, such as $U = \begin{cases} 0\,,\ if\ r < 0.34 \\ 1\,,\ otherwise \end{cases}$.

3. MPSOGOA

The GOA possesses the advantage of finding effective solutions for most optimization problems. However, it is characterized by the drawback of low convergence accuracy and slow convergence speed. This paper addresses this issue from three perspectives: introducing a chaotic strategy to enhance the quality of initial solutions; implementing population-wide perturbation to improve the convergence speed in the early iterations and the convergence accuracy in the later iterations; and integrating PSO to emphasize the significance of individual gazelle experiences, effectively balancing the exploration and exploitation aspects of the algorithm.

3.1. Chaos Strategy

Chaotic motion is non-repetitive and has characteristics of randomness and ergodicity. In recent years, chaotic mapping has been used by many scholars [45–49] for optimization algorithms, and has achieved good results in improving population diversity. The initial population of the GOA when solving optimization problems is randomly generated data. The initial gazelle population generated using this method is uncertain, and individual gazelles cannot traverse the feasible region. The diversity and uniformity of the initial population will affect the optimization ability of the algorithm. Chaotic mapping has a higher search speed than random search, can prevent falling into local optimality when solving optimization problems, and improves the global search ability of the algorithm.

Reasonable use of chaos theory in the population initialization stage can evenly distribute population individuals within the feasible region, thereby achieving the purpose of improving population diversity and uniformity. Currently, many literatures use Logistic mapping, but the traversal of Logistic mapping is uneven, resulting in unsatisfactory convergence speed of the algorithm.

In this paper, Piecewise is used to map the initialized position of individual gazelles. Piecewise mapping produces uniform initial values within [0, 1] and performs better than Logistic mapping in terms of uniformity. Therefore, the Piecewise chaotic sequence can be introduced into the GOA, and the characteristics of the chaotic sequence can be used to effectively improve the ability of the GOA to search for the optimal solution. Its expression is given by Equation (13):

$$x(t+1) = \begin{cases} \frac{x(t)}{p}, & 0 \le x(t) < p \\ \frac{x(t)-p}{0.5-p}, & p \le x(t) < 0.5 \\ \frac{1-p-x(t)}{0.5-p}, & 0.5 \le x(t) < 1-p \\ \frac{1-x(t)}{p}, & 1-p \le x(t) < 1 \end{cases} \tag{13}$$

The number of iterations is set to 1000, and the distribution histogram and scatter plot of the generated PLCM and Logistic mapping are shown in Figure 1. It can be seen from the diagram that the initial gazelle population based on PLCM chaotic map is more evenly distributed, avoiding the situation of focusing on a certain point, and avoiding the distribution characteristics of large at both ends and small in the middle presented by Logistic map.

3.2. Global Perturbation of the Population

The gazelle matrix represents the positions of individual gazelles, and the optimization of the positions of individual gazelles can be achieved by perturbing the gazelle matrix. By perturbing the gazelle matrix, we can effectively optimize the positions of individual gazelles, thereby enhancing the convergence speed of the algorithm in the initial iterations. Furthermore, this perturbation also increases the capability of the algorithm to escape from local optima in the later iterations, making the algorithm more adept at global searches. In the GOA, the perturbation of the gazelle matrix is typically achieved by randomly selecting and updating the positions of individual gazelles. This randomness helps break the possibility of the algorithm getting trapped in local optima, enabling the algorithm to search for better solutions in a larger search space. The mathematical model for the population-wide perturbation is provided by Equations (14) and (15):

$$new\_gazelle_{t+1} = \begin{cases} gazelle_t + r \cdot (RANDOM - P \cdot gazelle_t) & if \ \mathrm{F}_{RANDOM} < \ \mathrm{F}_{gazelle_t} \\ gazelle_t + r \cdot (gazelle_t - RANDOM) & \text{else} \end{cases} \tag{14}$$

$$gazelle_{t+1} = \begin{cases} new\_gazelle_{t+1} & if \ \mathrm{F}_{new_t} < \ \mathrm{F}_{gazelle_t} \\ gazelle_t & \text{else} \end{cases} \tag{15}$$

where gazelle$_t$ represents the positions at the t-th iterations, $\mathrm{F}_{gazelle_t}$ is its corresponding fitness value, $new\_gazelle_{t+1}$ represents the temporary position of the (t + 1)-th iterations, F_{newt} is its corresponding fitness value, r is a random number within the range [0, 1], P is a coefficient factor of 1 or 2, RANDOM denotes the position of a randomly selected gazelle individual in the population, and FRANDOM is its corresponding fitness value.

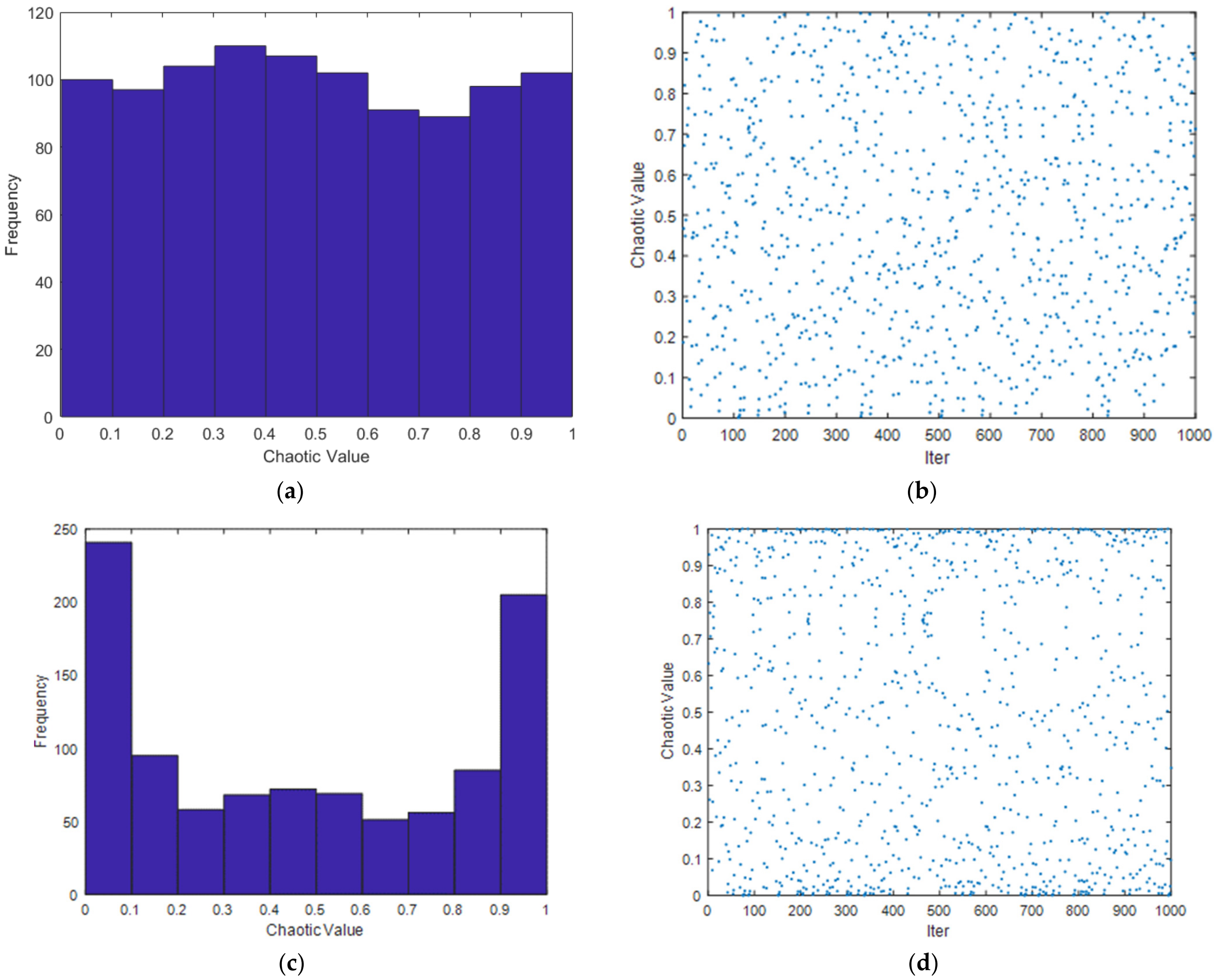

Figure 1. Piecewise mapping distribution plot and histogram. (**a**) Piecewise mapping distribution histogram; (**b**) Piecewise mapping distribution scatter plot; (**c**) Logistic map distribution histogram; (**d**) Logistic mapping distribution scatter plot.

3.3. Combined with PSO

3.3.1. PSO

The PSO algorithm [50] is a population-based stochastic search algorithm that mimics the social behavior of birds during foraging. It seeks the optimal solution in the solution space using two attributes: velocity and position. Throughout the iterative process of the algorithm, each particle in the population represents a candidate solution. The best position (pbest) of each particle, as well as the global best position (gbest) of the population, are recorded to find the optimal solution for the optimization problem.

Suppose the PSO algorithm is applied to an optimization problem in a d-dimensional search space. The updated equations for the j-th dimension velocity component $v_{i,j}$ and the position component $x_{i,j}$ of the i-th particle $x_i = (x_{i,1}, x_{i,2}, \ldots, x_{i,d})$ in the t + 1th iteration of the population are given by:

$$\begin{cases} v_{t+1} = \omega \cdot v_t + c_1 rand_1(pbest_t - x_t) + c_2 rand_2(gbest - x_t) \\ x_{t+1} = x_t + v_{t+1} \end{cases} \tag{16}$$

where ω represents the inertia weight, c_1 and c_2 are acceleration factors, and $rand_1$ and $rand_2$ are uniformly distributed random numbers in the range [0, 1].

3.3.2. Combination of PSO and GOA

Combining the two optimization algorithms has become a mainstream trend, and many scholars have shown that this approach can achieve remarkable results. This fusion not only strengthens the overall performance of the algorithm, but also cleverly makes up for the limitations of a single algorithm and realizes the complementarity and enhancement of advantages. The combination of GOA and PSO algorithm provides a new effective method to deal with complex optimization problems. In the PSO algorithm, the position update of particles mainly depends on the historical best position information of individuals and groups. The GOA simulates the behavior of gazelles in nature when they escape from predators. The core formula of gazelle position renewal includes Equations (3), (8) and (10), all of which indicate that gazelle position renewal depends mainly on the guidance and influence of the best gazelle individual. If the best gazelle individual chooses the wrong escape route, it will lead the population to extinction. In the optimization problem, the choice of the best gazelle individual and its escape route are mapped to the search process of the optimal solution in the algorithm, then the choice of the wrong escape route by the best gazelle individual is equivalent to the algorithm falling into the local optimal solution or misleading solution in the search process. In this case, the whole population (that is, the search space of the algorithm) may be affected by this wrong solution, resulting in the whole search process deviating from the direction of the global optimal solution, and ultimately getting unsatisfactory optimization results. If the concept of individual escape experience is introduced into the GOA, even if the best gazelle individual accidentally falls into the local optimal solution, other gazelle individuals can still escape from the local solution by relying on their individual escape experience. The combined method can be modeled using Equation (17), and the positions and velocities of particles can also be updated,

$$\begin{cases} v_{t+1} = \omega \cdot v_t + c_1 rand_1(pbest - gazelle_t) + c_2 rand_2(gbest - gazelle_t) \\ gazelle_{t+1} = gazelle_t + v_{t+1} \\ \omega = \omega_{\min} + (\omega_{\max} - \omega_{\min}) \cdot (T - t)/T \end{cases} \tag{17}$$

where $\omega_{\min}$ is the minimum inertia weight and $\omega_{\max}$ is the maximum inertia weight.

After combining PSO with GOA in the optimization process, it can not only learn from the wisdom of top gazelles, but can also make full use of the experience accumulated by individual gazelles in the escape process, which makes the whole population better jump out of the local optimal trap in the search process and enhances the search ability of the algorithm in the complex and changeable problem space. This fusion makes the excellent solution propagate and utilize in the population more quickly, accelerating the convergence speed of the whole population.

3.4. Pseudocode of the Proposed Algorithm

The pseudocode of the MPSOGOA outlines the process of the search optimization scheme as shown in Algorithm 1. The chaotic strategy improves the quality of the initial solutions, while the population-wide perturbation enhances the convergence speed and accuracy of the algorithm. Integration with PSO amplifies the role of individual experiences during the optimization process, preventing premature convergence of the algorithm. After meeting the termination conditions, the algorithm outputs the identified optimal solution. The combined action of the three strategies ensures both a high level of precision and an improved convergence speed of the optimization results, thereby guaranteeing that MPSOGOA can always find the optimal solution.

Algorithm 1 **Pseudocode of MPSOGOA**

```
Initialize algorithm parameters s, μ, S, PSRs, C1, C2.
Use Piecewise mapping to initialize the population.
While (iter < max_iter)
    Evaluate the fitness value of the gazelle. Construct pbest, gbest, and Elite.
    For each gazelle in the population:
        Generate a new gazelle matrix based on Equation (14).
        Update the gazelle matrix according to Equation (15).
    End For
    For each gazelle in the population:
        For each dimension:
            If (mod (iter, 2) = 0) then
                μ = −1
            Else
                μ = 1
            End If
            If (r > 0.5) then
                Execute exploration activities on the gazelle matrix according to Equation (3).
            Else
                If iter < size(gazelle,1)/2 then
                    Perform Brownian motion on the gazelle matrix according to Equation (10).
                Else
                    Execute Lévy flight on the gazelle matrix according to Equation (8).
                End If
            End If
        End For
    End For
Execute particle swarm movement on the gazelle matrix based on Equation (26).
Evaluate the fitness value of the gazelle.
Update pbest, gbest, and Elite.
Execute escape movement on the gazelle matrix according to Equation (12).
Iter = iter + 1
End While
Return the optimal value from the population.
```

According to the flowchart in Figure 2, the MPSOGOA process involves primarily initializing the population, evaluating the fitness of the gazelle, and updating candidate solutions. The complexity of MPSOGOA is determined by the maximum iteration count (iter_max), the population size (P), and the problem's dimension (D). From the algorithm flowchart, it is evident that the algorithm complexity is composed of two parts, denoted as O(iter_max × D) + O(F). Among these, F represents the time consumed by the algorithm in evaluating various functions. Thus, the complete analysis of algorithm complexity is as follows: O(MPSOGOA) = O(iter_max × P × D) + O(CFE × P). The complexity analysis of MPSOGOA can be simplified to: O(MPSOGOA) = O(iter_max × P × D + CFE × P).

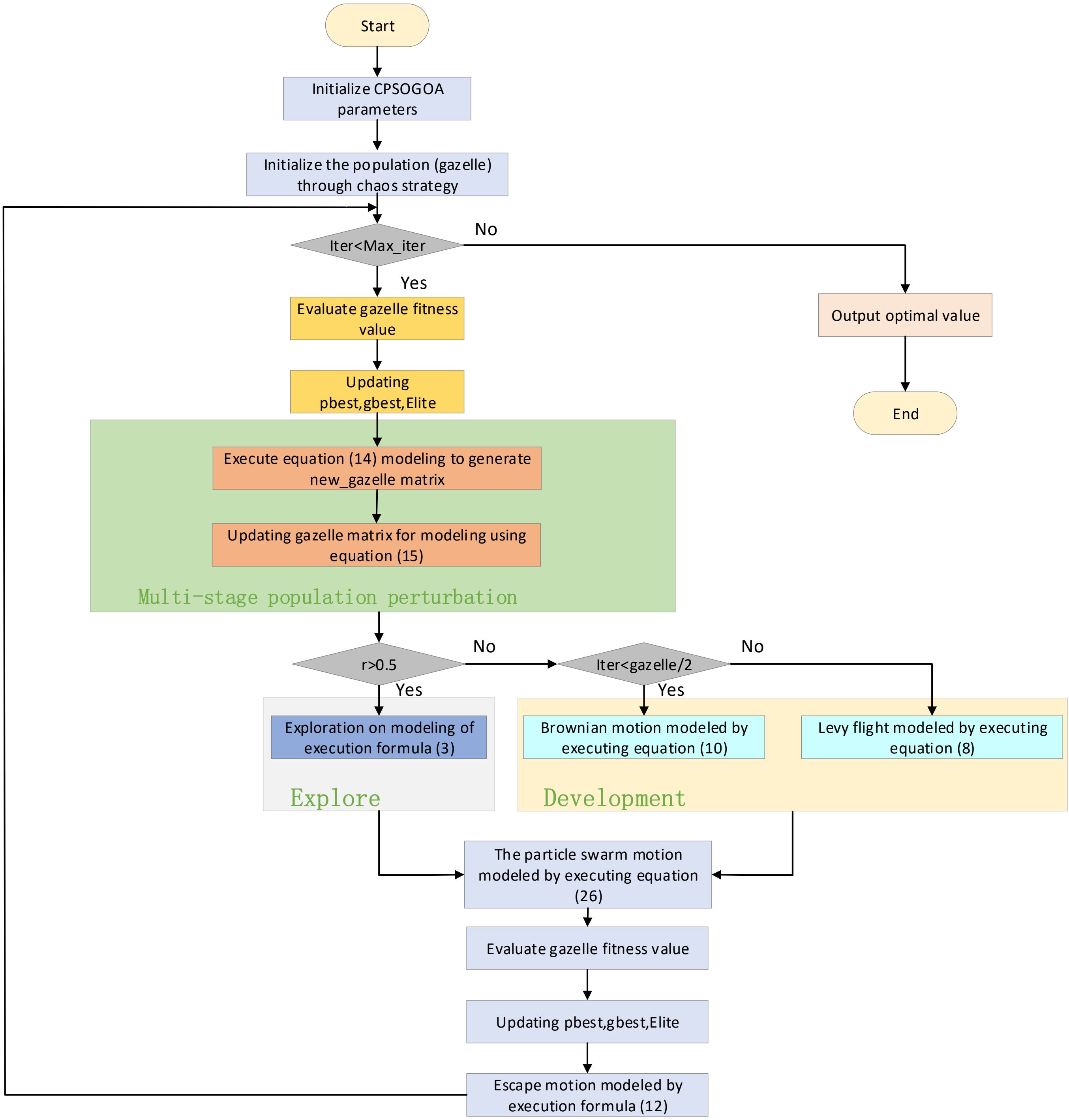
Start
Initialize CPSOGOA parameters
Initialize the population (gazelle) through chaos strategy
Iter<Max_iter
No
Yes
Evaluate gazelle fitness value
Updating pbest,gbest,Elite
Output optimal value
End
Execute equation (14) modeling to generate new_gazelle matrix
Updating gazelle matrix for modeling using equation (15)
Multi-stage population perturbation
r>0.5
No
Yes
Iter<gazelle/2
No
Yes
Exploration on modeling of execution formula (3)
Brownian motion modeled by executing equation (10)
Levy flight modeled by executing equation (8)
Explore
Development
The particle swarm motion modeled by executing equation (26)
Evaluate gazelle fitness value
Updating pbest,gbest,Elite
Escape motion modeled by execution formula (12)

Figure 2. MPSOGOA flow chart.

4. Experimental Design

This section presents an analysis of the simulation results of the MPSOGOA. The performance of the proposed MPSOGOA is evaluated using 35 test functions and 4 practical engineering design problems. The results of MPSOGOA in test functions and practical engineering applications are compared with the following algorithms: MPSOGOA, GOA, grey wolf optimizer (GWO) [51], sine cosine algorithm (SCA) [52], arithmetic optimization algorithm (AOA) [53], PSO [50], differential evolution (DE) [54], chimp optimization algorithm (Chimp) [55], biogeography-based optimization (BBO) [56], and golden jackal optimization (GJO) [57]. All experiments were conducted on a computer running on a

64-bit Windows 7 operating system equipped with a Core i5 CPU operating at a frequency of 2.50 GHz and 4.0 GB of RAM. The Matlab version used was R2021b. To minimize the impact of randomness on the algorithm, all algorithms were independently run 30 times for each test function, with the population size (P) set to 50 and the maximum iteration count (iter_max) set to 1000 generations. The parameter settings for all algorithms in the experiment are shown in Table 1.

Table 1. Algorithm parameter settings for comparison.

Algorithm	Parameter	Parameter Value
GOA	PSRs	0.34
	S	0.88
GWO	a	[0, 2]
	r1f r2	[0, 1]
SCA	a	2
AOA	α	5
	μ	0.05
PSO	C1, C2	2
	Wmax	0.9
	Wmin	0.2
DE	Lower bound of scale factor	0.2
	Upper bound of scale factor	0.8
BBO	nKeep	0.2
	Pmutation	0.9

To comprehensively evaluate the effectiveness of the algorithm, the following statistical evaluation indicators are utilized: best value, worst value, mean value, standard deviation (SD), and median value.

4.1. Test Function

Tables 2 and 3 record the 35 test functions used to evaluate the performance of the MPSOGOA. The first 20 problems are classic test functions in optimization problems. Table 2 provides the test functions, their positions, and the corresponding optimal values. F1–F5 are continuous unimodal functions. F6 represents a discontinuous step function, while F7 denotes a quartic noise function. F8–F13 are multimodal functions, and F14–F20 are fixed-dimension multimodal functions. Table 3 presents 15 problems, including a selection of test functions from the CEC2014 and CEC2017 competitions. F21 and F22 are unimodal functions, F23–F31 and F35 are simple multimodal functions, and F34 represents a hybrid function. Unimodal functions typically have a single global optimum and are often used to test the exploratory capabilities of metaheuristic algorithms. Multimodal functions have multiple local optima, making them more complex than unimodal functions. Therefore, they are frequently employed to test whether optimization techniques possess good exploratory capabilities. The number of multimodal functions exponentially increases with the design variables, balancing exploration and exploitation to enhance the algorithm’s search efficiency and prevent it from getting trapped in local optima. These test functions are used to infer the potential for the algorithm to find optimal solutions in real-world problems.

Table 2. Classic test function.

ID	Function	Dim	Range	Global
F1	$f(x) = \sum\limits_{i=1}^{n} x_i^2$	30	$[-100, 100]$	0
F2	$f(x) = \sum\limits_{i=0}^{n} \lvert x_i \rvert + \prod\limits_{i=0}^{n} \lvert x_i \rvert$	30	$[-10, 10]$	0
F3	$f(x) = \sum\limits_{i=1}^{d} \left(\sum\limits_{j=1}^{i} x_j \right)^2$	30	$[-100, 100]$	0
F4	$f(x) = \max_i\{\lvert x_i \rvert, 1 \le i \le n\}$	30	$[-100, 100]$	0
F5	$f(x) = \sum\limits_{i=1}^{n-1} \left[100(x_i - x_{i+1})^2 + (1 - x_i)^2 \right]$	30	$[-30, 30]$	0
F6	$f(x) = \sum\limits_{i=1}^{n} ([x_i - 0.5])^2$	30	$[-100, 100]$	0
F7	$f(x) = \sum\limits_{i=1}^{n} i x_1^4 + rand[0, 1)$	30	$[-128, 128]$	0
F8	$f(x) = \sum\limits_{i=1}^{n} -x_i \sin(\sqrt{\lvert x_i \rvert})$	30	$[-500, 500]$	418.9829 Dim
F9	$f(x) = 10 + \sum\limits_{i=1}^{n} (x_i^2 - 10\cos(2\pi x_i))$	30	$[-5.12, 5.12]$	0
F10	$f(x) = -a \exp\left(-0.02\sqrt{n^{-1} \sum\limits_{i=1}^{n} x_i^2} \right) - \exp\left(n^{-1} \sum\limits_{i=1}^{n} \cos(2\pi x_i) \right) + a + e, a = 20$	30	$[-32, 32]$	0
F11	$f(X) = 1 + \frac{1}{4000} \sum\limits_{i=1}^{n} x_i^2 - \prod\limits_{i=1}^{n} \cos\left(\frac{x_i}{\sqrt{i}} \right)$	30	$[-600, 600]$	0
F12	$f(x) = \frac{\pi}{n}\{10\sin(\pi y_i)\} + \sum\limits_{i=1}^{n} (y_i - 1)^2 \left[1 + 10\sin^2(\pi y_{i+1}) + \sum\limits_{i=1}^{n} u(x_i, 10, 100, 4) \right],$ $y_i - 1 + \frac{x_i+1}{4}, u(x_i, a, k, m) \begin{cases} K(x_i - a)^m & if x_i > a \\ 0 & -\mathrm{a} \le x_i \ge a \\ K(-x_i - a)^m & -\mathrm{a} \le x_i \end{cases}$	30	$[-50, 50]$	0
F13	$f(x) =$ $0.1\left(\sin^2(3\pi x_1) + \sum\limits_{i=1}^{n} (x_i - 1)^2 [1 + \sin^2(3\pi x_i + 1)] + (x_n - 1)^2 [1 + \sin^2(2\pi x_n)] \right) +$ $\sum\limits_{i=1}^{n} u(x_i, 5, 100, 4)$	30	$[-50, 50]$	0
F14	$f(x) = \left(\frac{1}{500} + \sum_{j=1}^{25} \frac{1}{j + \sum_{i=1}^{2} \left(x_j - a_{ij} \right)^6} \right)^{-1}$	2	$[-65, 65]$	1
F15	$f(x) = \sum\limits_{i=1}^{11} \left[a_i - \frac{x_1(b_i^2 + b_i x_2)}{b_i^2 + b_i x_3 + x_4} \right]^2$	4	$[-5, 5]$	0.00030
F16	$f(x) = 4x_1^2 - 2.1x_1^4 + \frac{1}{3}x_1^6 + x_1 x_2 - 4x_2^2 + 4x_2^4$	2	$[-5, 5]$	-1.0316
F17	$f(x) = \left(x_2 - \frac{5.1}{4\pi^2} x_1^2 + \frac{5}{\pi} x_1 - 6 \right)^2 + 10\left(1 - \frac{1}{8\pi} \right) \cos x_1 + 10$	2	$[-5, 5]$	0.398
F18	$f(x) = [1 + (x_1 + x_2 + 1)^2 (19 - 14x_1 + 3x_1^2 - 14x_2 + 6x_1 x_2 + 3x_2^2)]$ $\times [30 + (2x_1 - 3x_2)^2 (18 - 32x_1 + 12x_1^2 + 48x_2 - 36x_1 x_2 + 27x_2^2)]$	2	$[-2, 2]$	3
F19	$f(x) = -\sum_{i=1}^{4} c_1 \exp(-\sum_{j=1}^{3} a_{ij}(x_j - p_{ij})^2)$	3	$[1, 3]$	-3.86
F20	$f(x) = -\sum_{i=1}^{4} c_1 \exp(-\sum_{j=1}^{3} a_{ij}(x_j - p_{ij})^2)$	6	$[0, 1]$	-3.32

Table 3. CEC2014 and CEC2017 combined test functions.

ID	Function	F_i
F21	Rotated High Conditioned Elliptic Function (CEC 2014 F1)	100
F22	Shifted and Rotated Bent Cigar Function (CEC 2017 F1)	100
F23	Shifted and Rotated Rosenbrock's Function (CEC 2017 F3)	300
F24	Shifted and Rotated Rastrigin's Function (CEC 2017 F4)	400
F25	Shifted and Rotated Expanded Scaffer's F6 Function (CEC 2017 F5)	500
F26	Shifted and Rotated Weierstrass Function (CEC 2014 F6)	600
F27	Shifted and Rotated Lunacek Bi_ Rastrigin Function (CEC 2017 F6)	600
F28	Shifted and Rotated Non-Continuous Rastrigin'sFunction (CEC 2017 F7)	700
F29	Shifted Rastrigin's Function (CEC 2014 F8)	800
F30	Shifted and Rotated Levy Function (CEC 2017 F8)	800
F31	Shifted and Rotated Schwefel's Function (CEC 2017 F9)	900
F32	Shifted Schwefel's Function (CEC 2014 F10)	1000
F33	Shifted and Rotated Schwefel's Function (CEC 2014 F11)	1100
F34	Hybrid Function 2 (n = 3) (CEC 2017 F11)	1100
F35	Shifted and Rotated Expanded Scaffers F6 Function (CEC 2014 F16)	1600

4.2. Practical Engineering Applications

By testing the performance of optimization techniques on real-world engineering problems and designing corresponding parameter values, the overall design cost is minimized. This study focuses on the welding beam design problem, compression spring design problem, and pressure vessel design problem in mechanical engineering. Most engineering design problems in practical applications are governed by equality and inequality constraints, which are managed in the design objective function using penalty functions. The application of MPSOGOA to mechanical engineering design problems is compared with results obtained from nine other metaheuristic algorithms.

4.2.1. Welded Beam

Welded beam design is a problem of minimizing optimization, often utilized to assess the capability of optimization techniques in addressing practical issues. The welded beam design involves the manufacturing of a welded beam with the minimum cost under multiple constraints. The proposed MPSOGOA, along with 10 other metaheuristic algorithms, is applied to the welded beam design problem to minimize the cost of manufacturing the welded beam. Figure 3 provides an illustration of the welded beam. The decision variables that constrain the minimization of the cost of the welded beam design include the length (l), height (h), thickness (b), and weld thickness (h) of the steel bars. The constraints for the welded beam design encompass shear force (τ), bending stress (θ), column buckling load (P_c), beam deflection (δ), and lateral constraints, represented by WBD constraints. The objective function and penalty function for this problem is as follows:

$$\min f(x_1, x_2, x_3, x_4) = 1.1047x_1^2x_2 + 0.04811x_3x_4(14 + x_2) \tag{18}$$

$$\begin{bmatrix} x_1 \\ x_2 \\ x_3 \\ x_4 \end{bmatrix} = \begin{bmatrix} h \\ l \\ t \\ b \end{bmatrix} \tag{19}$$

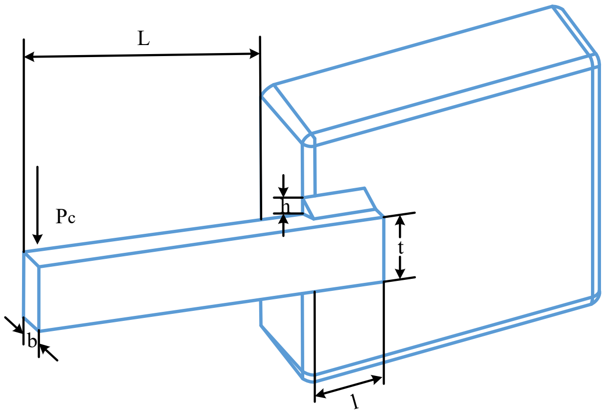

Figure 3. Schematic diagram of welded beam design.

The bounds of the variables are as follows:

$$\begin{cases} 0.1 \leq x_1 \leq 2.0 \\ 0.1 \leq x_2 \leq 10.0 \\ 0.1 \leq x_3 \leq 10.0 \\ 0.1 \leq x_4 \leq 2.0 \end{cases} \tag{20}$$

The constraints are as follows:

$$\begin{cases} g_1(\overrightarrow{x}) = \tau(\overrightarrow{x}) - \tau_{\max} \leq 0 \\ g_2(\overrightarrow{x}) = \sigma(\overrightarrow{x}) - \sigma_{\max} \leq 0 \\ g_3(\overrightarrow{x}) = \delta(\overrightarrow{x}) - \delta_{\max} \leq 0 \\ g_4(\overrightarrow{x}) = x_1 - x_4 \leq 0 \\ g_5(\overrightarrow{x}) = P - P_c(\overrightarrow{x}) \leq 0 \\ g_6(\overrightarrow{x}) = 0.125 - x_1 \leq 0 \\ g_7(\overrightarrow{x}) = 1.10471x_1^2x_2 + 0.04811x_3x_4(14 + x_2) - 5 \leq 0 \end{cases} \tag{21}$$

The intermediate variables of the constraints are as follows:

$$\begin{aligned} &\tau(\overrightarrow{x}) = \sqrt{(\tau')^2 + 2\tau'\tau''\tfrac{x_2}{2R} + (\tau'')^2} \\ &\tau' = \tfrac{P}{\sqrt{2}x_1x_2} \\ &\tau'' = \tfrac{MR}{J} \\ &M = P(L + 0.5x_2) \\ &R = \sqrt{0.25(x_2^2 + (x_1 + x_3)^2)} \\ &J = 2(x_1x_2\sqrt{2}(\tfrac{x_2^2}{12} + \tfrac{(x_1+x_2)^2}{4})) \\ &\sigma(\overrightarrow{x}) = \tfrac{6PL}{x_4x_3^2} \\ &\delta(\overrightarrow{x}) = \tfrac{6PL^3}{Ex_3^2x_4} \\ &P_c = \tfrac{4.013E}{L^2}\sqrt{\tfrac{x_3^2x_4^6}{36}}(1 - \tfrac{x_3}{2L}\sqrt{\tfrac{E}{4G}}) \end{aligned} \tag{22}$$

where $\sigma_{\max}$ = 3 × 10^4 psi, P = 6 × 10^3 lb, L = 14 in, $\delta_{\max}$ = 0.25 in, E = 30 × 10^6 psi, $\tau_{\max}$ = 13600 psi, and G = 1.2 × 10^7 psi.

4.2.2. Compression Spring Design Issues

The objective of spring design is to minimize the total weight of the tension/compression spring. As depicted in Figure 4, this spring design problem is controlled by three parameters: the wire diameter (d), mean coil diameter (D), and number of active coils in the spring (P). The design function and constraint function for the spring design problem are given in Equations (24) and (25),

$$l = \begin{bmatrix} l_1 \\ l_2 \\ l_3 \end{bmatrix} = \begin{bmatrix} d \\ D \\ P \end{bmatrix} \tag{23}$$

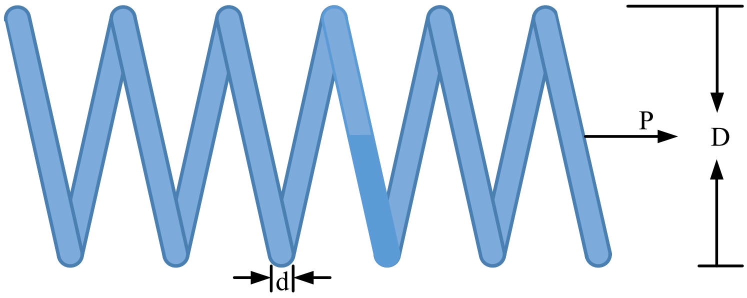

Figure 4. Schematic diagram of compression spring design problem.

The boundary conditions of the variables are as follows:

$$\begin{cases} 0.05 \leq l_1 \leq 2 \\ 0.25 \leq l_2 \leq 1.3 \\ 2 \leq l_3 \leq 15 \end{cases} \tag{24}$$

$$Minimize f(l) = (l_3 + 2)l_2 l_1^2 \tag{25}$$

The constraints of the spring design problem are as follows:

$$s.t.\begin{cases} g_1(\vec{l}\,) = 1 - \frac{l_2^3 l_3}{71785 l_1^4} \le 0 \\ g_2(\vec{l}\,) = \frac{4l_2^2 - l_1 l_2}{12566(l_3 l_1^3 - l_1^4)} + \frac{1}{5108 l_1^2} \le 0 \\ g_3(\vec{l}\,) = 1 - \frac{140.45 l_1}{l_2^2 l_3} \le 0 \\ g_4(\vec{l}\,) = \frac{l_1 + l_2}{1.5} - 1 \le 0 \end{cases} \tag{26}$$

4.2.3. Pressure Vessel Design

The primary objective of the pressure vessel design problem is to minimize the production cost of the pressure vessel to the greatest extent possible (Figure 5). This problem is governed by four control parameters: the thickness of the pressure vessel (Ts), thickness of the head (Th), internal radius of the vessel (R), and length of the vessel head (L). The design function and constraint function for the pressure vessel design problem are provided in Equations (29) and (30), respectively,

$$x = \begin{bmatrix} l_1 \\ l_2 \\ l_3 \\ l_4 \end{bmatrix} = \begin{bmatrix} T_s \\ T_h \\ R \\ L \end{bmatrix} \tag{27}$$

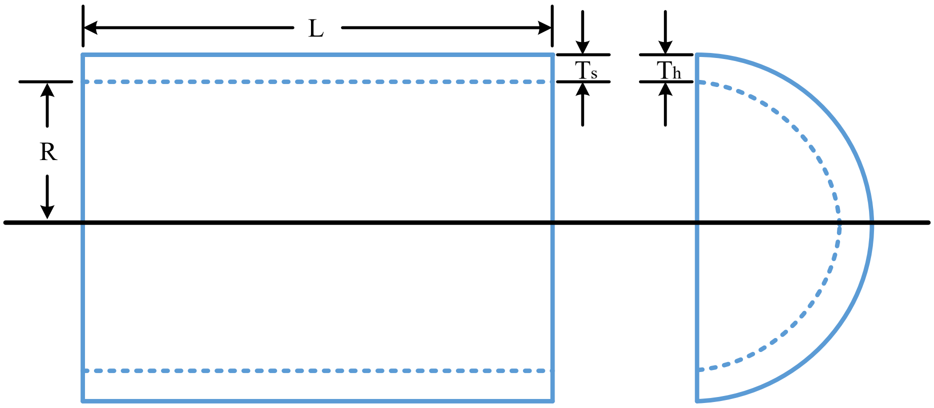

Figure 5. Schematic diagram of pressure vessel design issues.

The variation range of variables is as follows:

$$\begin{cases} 0 \le l_1 \le 99 \\ 0 \le l_2 \le 99 \\ 10 \le l_3 \le 200 \\ 10 \le l_4 \le 200 \end{cases} \tag{28}$$

$$Minimize f(x) = 0.6224 l_1 l_3 l_4 + 1.7781 l_2 l_3^2 + 3.1661 l_1^2 l_4 + 19.84 l_1^2 l_3 \tag{29}$$

The constraints of the pressure vessel design problem are as follows:

$$s.t.\begin{cases} g_1(\vec{l}\,) = -l_1 + 0.0193 l_3 \le 0 \\ g_2(\vec{l}\,) = -l_2 + 0.00954 l_3 \le 0 \\ g_3(\vec{l}\,) = -\pi l_3^2 l_4 - \frac{4}{3}\pi l_3^3 + 1296000 \le 0 \\ g_4(\vec{l}\,) = l_4 - 240 \le 0 \end{cases} \tag{30}$$

5. Results and Discussion

In this section, to validate the performance of the proposed MPSOGOA, 35 test functions and 3 real-world engineering optimization problems are employed for performance testing, and comparisons are made with the original GOA and currently popular metaheuristic algorithms. The entire experiment is conducted in the following parts: (1) analysis of the experimental results of classical test functions, (2) analysis of the experimental results of the CEC2014 and CEC2017 composite test functions, (3) convergence performance of the MPSOGOA, and (4) result analysis of the 3 engineering optimization problems.

The performance of each algorithm is measured using five performance indicators: best value, worst value, average value, standard deviation, and median. Furthermore, the performance of the MPSOGOA is evaluated using Friedman rank sum test and Wilcoxon signed-rank test.

5.1. Test Function Results

5.1.1. Analysis of CEC2005 Experimental Results

Table 4 presents the experimental results of 10 algorithms on 20 benchmark functions, including the best results obtained from 30 independent runs (Best), the worst results (Worst), the mean values (Mean), the standard deviations (Std), the medians (Median), and the Wilcoxon signed-rank test rankings (Rank) of each algorithm across the 20 benchmark functions. The final ranking is determined by the Friedman rank sum ranking of each algorithm across the 20 benchmark functions.

Unimodal functions have only one optimal value, so they are often used to test the exploitation capability of algorithms. It can be seen from Table 4 that MPSOGOA shows the best performance on F1–F4. When solving F1, the convergence accuracy is improved by 180 orders of magnitude compared with GOA and 61 orders of magnitude compared with other algorithms. The convergence accuracy is also improved in different degrees. When solving F2, F3, and F4, the convergence accuracy is improved by more than 57 orders of magnitude and the standard deviation is improved by more than 40 orders of magnitude compared with GOA. Compared with GOA on F5–F7, the optimum values are improved. There is an improvement of two orders of magnitude on F6 and one order of magnitude on F7, with a smaller standard deviation. This means that the stability is also improved while the accuracy of convergence is improved. The above results indicate that MPSOGOA has good exploitation capability. F8–F20 is a multimodal function and a fixed-dimensional multimodal function, which usually has multiple extreme values and is often used to test the exploration ability of the algorithm. In the test of multimodal functions F8–F13, MPSOGOA performs better than other comparison algorithms on most functions and can find the optimal solution. When solving F12 and F13, the convergence accuracy of MPSOGOA is improved by two orders of magnitude compared with GOA. MPSOGOA shows excellent exploration ability on multimodal functions. In the test of F14 and F15, the optimal value of MPSOGOA is similar to other algorithms, but its standard deviation is lower. The experimental results show that MPSOGOA has good performance in solving unimodal and multimodal functions and excellent performance in convergence accuracy and stability.

Table 5 shows the Friedman rankings of the 10 algorithms in the benchmark test function. MPSOGOA achieved good results in the Friedman test. The MPSOGOA proposed in this article ranks first among the 10 optimization algorithms.

Table 4. CEC2005 test results.

Function	Value	MPSOGOA	GOA	GWO	SCA	AOA	PSO	DE	Chimp	BBO	GJO
F1	Best	2.7433×10^{-268}	2.89154×10^{-88}	8.50069×10^{-73}	2.54974×10^{-8}	1.0643×10^{-207}	9.47085×10^{-12}	51.648	1.3579×10^{-27}	0.324489	1.2726×10^{-132}
	Worst	1.5559×10^{-214}	3.40688×10^{-24}	1.00555×10^{-69}	0.0243454	2.9067×10^{-95}	9.19223×10^{-8}	261.883	2.01606×10^{-18}	1.18724	5.5191×10^{-127}
	Average	5.1864×10^{-216}	1.13563×10^{-25}	1.63935×10^{-70}	0.0013788	2.59489×10^{-96}	3.99524×10^{-9}	131.843	2.11538×10^{-19}	0.619129	5.5742×10^{-128}
	SD	0	6.22009×10^{-25}	2.59621×10^{-70}	0.00450527	7.96026×10^{-96}	1.66386×10^{-8}	49.421	5.13648×10^{-19}	0.166653	1.3812×10^{-127}
	Median	5.0964×10^{-252}	5.30668×10^{-78}	5.55451×10^{-71}	8.70929×10^{-5}	8.3471×10^{-131}	6.60832×10^{-10}	124.27	2.16579×10^{-22}	0.579377	9.8842×10^{-130}
F2	Best	1.5987×10^{-137}	9.12414×10^{-57}	9.04044×10^{-42}	9.4068×10^{-09}	0	6.63994×10^{-7}	18.9427	8.76387×10^{-19}	0.158091	6.77923×10^{-76}
	Worst	1.006×10^{-117}	1.5473×10^{-20}	4.17611×10^{-40}	6.56174×10^{-5}	1.3602×10^{-129}	177.155	55.6008	1.66733×10^{-12}	0.318038	6.08005×10^{-73}
	Average	3.3535×10^{-119}	5.58832×10^{-22}	6.87572×10^{-41}	4.5299×10^{-6}	4.5341×10^{-131}	5.90526	41.1955	1.32586×10^{-13}	0.245152	6.65278×10^{-74}
	SD	1.8366×10^{-118}	2.82639×10^{-21}	9.28251×10^{-41}	1.25192×10^{-5}	2.4834×10^{-130}	32.3439	9.34487	3.44014×10^{-13}	0.0386638	1.37309×10^{-73}
	Median	6.7837×10^{-133}	7.41398×10^{-49}	3.6684×10^{-41}	4.08327×10^{-7}	5.8246×10^{-210}	1.47627×10^{-5}	42.7029	1.31203×10^{-14}	0.251466	1.30119×10^{-74}
F3	Best	4.35826×10^{-69}	2.63083×10^{-12}	2.90856×10^{-24}	27.8478	0	236.094	22,892.9	6.69748×10^{-10}	34.0053	2.07975×10^{-58}
	Worst	4.07582×10^{-43}	0.00307754	3.26631×10^{-17}	10,369.5	2.50525×10^{-45}	2541.13	38,833.8	0.019964	147.677	1.01149×10^{-43}
	Average	1.40494×10^{-44}	0.00021169	2.07546×10^{-18}	2522.16	8.35084×10^{-47}	929.7	29,602.2	0.0010311	85.0581	3.37788×10^{-45}
	SD	7.4369×10^{-44}	0.00062157	7.24266×10^{-18}	2409.21	4.57394×10^{-46}	484.589	4207.89	0.00363366	31.1403	1.84661×10^{-44}
	Median	7.55093×10^{-62}	1.02692×10^{-7}	1.63874×10^{-21}	1486.21	2.2905×10^{-102}	889.357	28,564	4.07225×10^{-5}	77.9158	7.89966×10^{-50}
F4	Best	1.9656×10^{-108}	3.9303×10^{-28}	9.91516×10^{-19}	0.929186	1.03144×10^{-73}	3.18226	43.3947	6.74566×10^{-7}	0.554326	1.03235×10^{-41}
	Worst	1.70792×10^{-81}	3.0358×10^{-9}	2.82651×10^{-16}	49.1954	5.65999×10^{-24}	13.1182	79.2222	0.00700025	0.976223	7.45118×10^{-37}
	Average	5.69308×10^{-83}	1.68167×10^{-10}	2.73887×10^{-17}	18.2135	1.88688×10^{-25}	6.51546	60.02	0.00044706	0.793745	3.86938×10^{-38}
	SD	3.11823×10^{-82}	5.9787×10^{-10}	5.608×10^{-17}	12.3822	1.03336×10^{-24}	2.42973	7.54042	0.00130382	0.10542	1.36229×10^{-37}
	Median	4.1655×10^{-104}	8.56731×10^{-22}	7.15996×10^{-18}	16.4155	1.13063×10^{-51}	5.70036	60.1497	6.26622×10^{-05}	0.79626	2.99064×10^{-39}
F5	Best	21.4468	22.9354	24.6847	27.5936	28.6067	8.56034	11,068.2	28.0816	31.1451	25.3295
	Worst	23.5746	24.4653	28.7236	1751.6	28.7969	661.168	108,590	28.9703	351.308	28.631
	Average	22.7803	23.6761	26.5531	142.032	28.6941	79.4806	41,419	28.8626	93.3473	27.1006
	SD	0.541546	0.335586	0.896212	323.732	0.0569614	119.223	22,907.2	0.218115	70.8855	0.720972
	Median	22.8075	23.6929	26.2039	41.667	28.6924	39.4477	36,874.4	28.9403	93.4376	27.1859
F6	Best	7.89475×10^{-5}	0.00241955	1.15757×10^{-5}	3.59634	4.84586	4.65703×10^{-11}	80.9834	2.03747	0.348594	1.25039
	Worst	0.0325062	0.0391195	1.23905	4.85133	5.64324	3.29787×10^{-8}	196.087	3.35535	1.01923	3.73296
	Average	0.00932258	0.0157147	0.413328	4.25324	5.25632	2.17583×10^{-9}	125.677	2.57539	0.628994	2.4552
	SD	0.00820061	0.0113896	0.284307	0.301315	0.200676	6.15369×10^{-9}	28.8418	0.367716	0.15143	0.547726
	Median	0.00713486	0.0118718	0.252159	4.27234	5.29563	5.46017×10^{-10}	117.846	2.61086	0.624407	2.50017
F7	Best	7.187×10^{-5}	0.00053906	0.00016618	0.00297477	2.47227×10^{-7}	0.0158195	0.0953463	2.13809×10^{-5}	0.00138442	4.75219×10^{-6}
	Worst	0.00195296	0.00364285	0.00109214	0.0454201	0.00018264	0.0754005	0.382486	0.00150594	0.00617976	0.00038551
	Average	0.00069391	0.00139031	0.00054627	0.0176046	2.62781×10^{-5}	0.0389288	0.228453	0.00049492	0.0034084	0.00011308
	SD	0.00041425	0.00079647	0.00021884	0.0105955	3.57008×10^{-5}	0.0137357	0.0611222	0.00039098	0.00092943	9.95327×10^{-5}
	Median	0.00061555	0.00114125	0.00048483	0.0142062	1.47276×10^{-5}	0.0371472	0.222044	0.00045812	0.00323732	6.96101×10^{-5}
F8	Best	−8138.49	−8515.22	−7424.74	−4468.92	−3828.82	−37,835.8	−5715.02	−5945.94	−10770.3	−7659.2
	Worst	−6975.58	−6920.39	−3296.85	−3572.19	−2443.18	−20,840.3	−4765.72	−5690.15	−7869.18	−2614.69
	Average	−7460.98	−7716.17	−6220.63	−3997.62	−3263.11	−29484.8	−5256.55	−5782.94	−8909.67	−4542.83
	SD	263.699	343.027	815.569	244.64	360.725	3770.12	234.332	60.4447	549.364	1181.45
	Median	−7428.94	−7655.97	−6340.2	−3970.16	−3347.24	−28,410.3	−5220.09	−5773.53	−8934.88	−4562.16
F9	Best	0	0	0	1.16642×10^{-5}	0	19.9018	209.2	0	16.1742	0
	Worst	0	0	3.22571	64.4795	0	65.6672	264.147	14.851	86.7699	0
	Average	0	0	0.214297	13.2237	0	38.7374	245.473	1.99373	36.9931	0
	SD	0	0	0.815539	20.1794	0	11.8587	13.1711	3.31979	14.1102	0
	Median	0	0	0	0.0824535	0	37.8085	246.993	1.51663×10^{-05}	36.1431	0
F10	Best	8.88178×10^{-16}	8.88178×10^{-16}	7.99361×10^{-15}	9.30212×10^{-5}	8.88178×10^{-16}	1.028×10^{-6}	19.1489	19.9571	0.151232	4.44089×10^{-15}
	Worst	4.44089×10^{-15}	4.44089×10^{-15}	1.5099×10^{-14}	20.2517	8.88178×10^{-16}	1.15515	19.9097	19.9633	0.317979	7.99361×10^{-15}
	Average	4.20404×10^{-15}	2.54611×10^{-15}	1.36779×10^{-14}	12.6514	8.88178×10^{-16}	0.115541	19.7291	19.961	0.233117	4.55932×10^{-15}
	SD	9.01352×10^{-16}	1.8027×10^{-15}	2.39689×10^{-15}	9.43353	0	0.35246	0.211468	0.00163427	0.0404489	6.48634×10^{-16}
	Median	4.44089×10^{-15}	8.88178×10^{-16}	1.5099×10^{-14}	20.0425	8.88178×10^{-16}	7.0606×10^{-6}	19.8274	19.9614	0.2293	4.44089×10^{-15}

Table 4. *Cont.*

Function	Value	MPSOGOA	GOA	GWO	SCA	AOA	PSO	DE	Chimp	BBO	GJO
F11	Best	0	0	0	9.0681×10^{-7}	0	1.86905×10^{-10}	1.32215	0	0.380873	0
	Worst	0	0	0.0130345	0.787373	1.36796×10^{-10}	0.0858724	2.83267	0.0562725	0.762887	0
	Average	0	0	0.00152591	0.194643	7.8508×10^{-12}	0.0149053	2.18131	0.013913	0.569153	0
	SD	0	0	0.00397392	0.247833	2.90085×10^{-11}	0.0209638	0.341406	0.0170819	0.0820724	0
	Median	0	0	0	0.0524653	0	0.00986098	2.17147	0.00516804	0.565946	0
F12	Best	2.26979×10^{-6}	0.00015077	1.02012×10^{-6}	0.362999	0.822674	1.96181×10^{-10}	26.1488	0.121075	0.00068518	0.0577601
	Worst	0.00088075	0.00165225	0.0705621	7.71822	0.985045	0.518258	12793.2	0.827538	0.00239739	0.293
	Average	0.00028298	0.00066260	0.0260683	0.977878	0.915726	0.0381841	1118.69	0.254804	0.00134462	0.162571
	SD	0.00024735	0.00041791	0.014828	1.35267	0.0395165	0.103529	2670.46	0.143964	0.00034593	0.0669722
	Median	0.00023877	0.00052306	0.0256778	0.587282	0.910336	3.41822×10^{-7}	44.9091	0.223983	0.00129926	0.16061
F13	Best	6.44767×10^{-6}	0.00193727	2.21166×10^{-5}	1.98426	2.69813	1.43267×10^{-10}	410.639	2.48256	0.0106384	1.13193
	Worst	0.0881833	0.0505603	0.612025	22.4576	2.9791	0.0439489	165937	2.99663	0.0377297	1.80974
	Average	0.0271388	0.0196544	0.256731	3.57318	2.9442	0.00402968	30,685.3	2.87568	0.0249777	1.49769
	SD	0.022066	0.0151691	0.138242	3.70598	0.0624779	0.00888511	37,310.4	0.12631	0.00791171	0.168996
	Median	0.0254443	0.0144074	0.278129	2.60472	2.97623	9.38257×10^{-8}	17,134.5	2.894	0.0249056	1.49676
F14	Best	0.998004	0.998004	0.998004	0.998004	0.998004	0.998004	0.998004	0.998004	0.998004	0.998004
	Worst	0.998004	0.998004	10.7632	2.98211	12.6705	0.998004	0.998004	0.998025	15.5038	12.6705
	Average	0.998004	0.998004	2.79612	1.52725	10.4761	0.998004	0.998004	0.998007	4.75683	3.80826
	SD	0	7.1417×10^{-17}	3.2852	0.89231	4.02764	0	0	4.58599×10^{-6}	3.91895	3.82079
	Median	0.998004	0.998004	0.998004	0.99805	12.6705	0.998004	0.998004	0.998005	3.96825	2.98211
F15	Best	0.00030748	0.00030748	0.00030748	0.00035615	0.00031508	0.00030748	0.00030748	0.00122912	0.00041479	0.00030749
	Worst	0.00030748	0.00030748	0.0208487	0.00145188	0.111842	0.00107688	0.00122317	0.00131389	0.0203633	0.00122336
	Average	0.00030748	0.00030748	0.00436536	0.00083847	0.0206497	0.00074842	0.00055166	0.00125336	0.00259708	0.00041668
	SD	1.84314×10^{-14}	6.92721×10^{-13}	0.00817898	0.00037638	0.0329258	0.00030631	0.00041185	2.14723×10^{-5}	0.00602555	0.00028961
	Median	0.00030748	0.00030748	0.00030749	0.00076172	0.00449986	0.00086359	0.00030748	0.00124767	0.00061481	0.00030753
F16	Best	−1.03163	−1.03163	−1.03163	−1.03163	−1.03163	−1.03163	−1.03163	−1.03163	−1.03163	−1.03163
	Worst	−1.03163	−1.03163	−1.03163	−1.03159	−1.03163	−1.03163	−1.03163	−1.03161	−1.03163	−1.03163
	Average	−1.03163	−1.03163	−1.03163	−1.03162	−1.03163	−1.03163	−1.03163	−1.03162	−1.03163	−1.03163
	SD	6.32085×10^{-16}	6.32085×10^{-16}	1.83844×10^{-9}	1.01345×10^{-5}	2.58411×10^{-11}	6.71219×10^{-16}	6.77522×10^{-16}	3.90178×10^{-6}	6.17114×10^{-16}	3.7554×10^{-8}
	Median	−1.03163	−1.03163	−1.03163	−1.03162	−1.03163	−1.03163	−1.03163	−1.03163	−1.03163	−1.03163
F17	Best	0.397887	0.397887	0.397887	0.397909	0.397889	0.397887	0.397887	0.397888	0.397887	0.397887
	Worst	0.397887	0.397887	0.397889	0.4004	0.398753	0.397887	0.397887	0.398964	0.397887	0.397937
	Average	0.397887	0.397887	0.397888	0.398542	0.398021	0.397887	0.397887	0.3981	0.397887	0.397893
	SD	0	0	4.12949×10^{-7}	0.00052226	0.00022284	0	0	0.00023883	4.16358×10^{-11}	9.20093×10^{-6}
	Median	0.397887	0.397887	0.397888	0.398434	0.397934	0.397887	0.397887	0.398006	0.397887	0.39789
F18	Best	3	3	3	3	3	3	3	3	3	3
	Worst	3	3	3.00001	3.00006	85.3767	3	3	3.00008	30	3.00001
	Average	3	3	3	3.00001	12.9459	3	3	3.00001	5.7	3
	SD	1.20918×10^{-15}	1.2452×10^{-15}	2.38556×10^{-6}	1.25267×10^{-5}	25.1878	5.83118×10^{-16}	1.72587×10^{-15}	1.90032×10^{-5}	8.23847	1.57663×10^{-6}
	Median	3	3	3	3	3	3	3	3.00001	3	3
F19	Best	−3.86278	−3.86278	−3.86278	−3.8624	−3.86266	−3.85208	−3.86278	−3.86237	−3.86278	−3.86278
	Worst	−3.86278	−3.86278	−3.85498	−3.8533	−3.8549	−3.03321	−3.86278	−3.85423	−3.86278	−3.85489
	Average	−3.86278	−3.86278	−3.86248	−3.85597	−3.86006	−3.66744	−3.86278	−3.85506	−3.86278	−3.85965
	SD	2.71009×10^{-15}	2.71009×10^{-15}	0.0014217	0.00276095	0.00258625	0.174799	2.71009×10^{-15}	0.0014238	2.36432×10^{-15}	0.00388555
	Median	−3.86278	−3.86278	−3.86278	−3.85483	−3.86138	−3.69565	−3.86278	−3.85477	−3.86278	−3.86275
F20	Best	3.322	−3.322	−3.32199	−3.13096	−3.29032	−2.27284	−3.322	−3.30839	−3.322	−3.32199
	Worst	−3.322	−3.322	−3.08391	−1.6919	−2.89712	−0.784013	−3.2031	−1.92068	−3.2031	−3.0156
	Average	−3.322	−3.322	−3.24742	−2.8927	−3.16648	−1.69532	−3.20707	−2.74374	−3.2784	−3.18099
	SD	1.48895×10^{-15}	4.29004×10^{-12}	0.0757351	0.36007	0.0731764	0.487457	0.0217068	0.370237	0.0582734	0.0828684
	Median	−3.322	−3.322	−3.20301	−3.01207	−3.17547	−1.68691	−3.2031	−2.79275	−3.322	−3.19719

Table 5. Friedman ranking of CEC2005.

Algorithm	Friedman Mean Rank	General Mean Rank
MPSOGOA	2.525	1
GOA	3.175	2
GWO	4.75	4
SCA	8.15	10
AOA	5.6	5
PSO	5.825	6
DE	7.55	9
Chimp	6.9	8
BBO	6.1	7
GJO	4.425	3

Furthermore, we conducted the Wilcoxon signed-rank test to assess the significance of differences between MPSOGOA and the other nine algorithms. When the *p*-value is less than 0.05, it is considered that there is a significant difference between the two algorithms for that specific function. The results of the Wilcoxon signed-rank test between MPSOGOA and the nine contrastive algorithms are presented in Table 6. It is evident from the table that MPSOGOA exhibits significant differences from the nine contrastive algorithms across the majority of the functions. Overall, across the 20 benchmark test functions, the performance of the MPSOGOA surpasses that of the nine contrastive algorithms, demonstrating strong competitiveness in the achieved results.

Table 6. Wilcoxon signed-rank test results for CEC2005.

Function	GOA	GWO	SCA	AOA	PSO	DE	Chimp	BBO	GJO
F1	3.01986×10^{-11}	3.01986×10^{-11}	3.01986×10^{-11}	3.01986×10^{-11}	3.01986×10^{-11}	3.01986×10^{-11}	3.01986×10^{-11}	3.01986×10^{-11}	3.01986×10^{-11}
F2	3.01986×10^{-11}	3.01986×10^{-11}	3.01986×10^{-11}	2.43954×10^{-10}	3.01986×10^{-11}	3.01986×10^{-11}	3.01986×10^{-11}	3.01986×10^{-11}	3.01986×10^{-11}
F3	3.01986×10^{-11}	3.01986×10^{-11}	3.01986×10^{-11}	2.0338×10^{-9}	3.01986×10^{-11}	3.01986×10^{-11}	3.01986×10^{-11}	3.01986×10^{-11}	7.65879×10^{-5}
F4	3.01986×10^{-11}	3.01986×10^{-11}	3.01986×10^{-11}	3.01986×10^{-11}	3.01986×10^{-11}	3.01986×10^{-11}	3.01986×10^{-11}	3.01986×10^{-11}	3.01986×10^{-11}
F5	4.57257×10^{-9}	3.01986×10^{-11}	3.01986×10^{-11}	3.01986×10^{-11}	8.84109×10^{-7}	3.01986×10^{-11}	3.01986×10^{-11}	3.01986×10^{-11}	3.01986×10^{-11}
F6	0.0223601	1.06657×10^{-7}	3.01986×10^{-11}	3.01986×10^{-11}	3.01986×10^{-11}	3.01986×10^{-11}	3.01986×10^{-11}	3.01986×10^{-11}	3.01986×10^{-11}
F7	6.2828×10^{-6}	0.185767	3.01986×10^{-11}	4.07716×10^{-11}	3.01986×10^{-11}	3.01986×10^{-11}	0.0518771	3.68973×10^{-11}	7.38029×10^{-10}
F8	0.000691252	1.41098×10^{-9}	3.01986×10^{-11}	3.01986×10^{-11}	3.01986×10^{-11}	3.01986×10^{-11}	3.01986×10^{-11}	4.97517×10^{-11}	3.4742×10^{-10}
F9	NaN	0.0215693	1.21178×10^{-12}	NaN	1.21178×10^{-12}	1.21178×10^{-12}	4.55563×10^{-12}	1.21178×10^{-12}	NaN
F10	9.55053×10^{-5}	6.53336×10^{-13}	2.36384×10^{-12}	7.15185×10^{-13}	2.36384×10^{-12}	2.36384×10^{-12}	2.36384×10^{-12}	2.36384×10^{-12}	0.0885796
F11	NaN	0.0419262	1.21178×10^{-12}	0.0419262	1.21178×10^{-12}	1.21178×10^{-12}	8.86583×10^{-7}	1.21178×10^{-12}	NaN
F12	5.97056×10^{-5}	5.57265×10^{-10}	3.01986×10^{-11}	3.01986×10^{-11}	0.0232434	3.01986×10^{-11}	3.01986×10^{-11}	4.50432×10^{-11}	3.01986×10^{-11}
F13	0.245814	5.57265×10^{-10}	3.01986×10^{-11}	3.01986×10^{-11}	4.68563×10^{-8}	3.01986×10^{-11}	3.01986×10^{-11}	0.923442	3.01986×10^{-11}
F14	0.0814042	1.21178×10^{-12}	1.21178×10^{-12}	1.20094×10^{-12}	NaN	NaN	1.21178×10^{-12}	4.4986×10^{-12}	1.21178×10^{-12}
F15	1.19287×10^{-6}	3.01608×10^{-11}	3.01608×10^{-11}	3.01608×10^{-11}	3.01608×10^{-11}	0.00192305	3.01608×10^{-11}	3.01608×10^{-11}	3.01608×10^{-11}
F16	1	7.57407×10^{-12}	7.57407×10^{-12}	7.57407×10^{-12}	0.0246374	0.00546603	7.57407×10^{-12}	5.21998×10^{-9}	7.57407×10^{-12}
F17	NaN	1.21178×10^{-12}	1.21178×10^{-12}	1.21178×10^{-12}	NaN	NaN	1.21178×10^{-12}	2.93292×10^{-5}	1.21178×10^{-12}
F18	0.690562	2.34656×10^{-11}	2.34656×10^{-11}	2.34505×10^{-11}	0.081759	1.63048×10^{-5}	2.34656×10^{-11}	2.56049×10^{-9}	2.34656×10^{-11}
F19	NaN	1.21178×10^{-12}	1.21178×10^{-12}	1.21178×10^{-12}	1.21178×10^{-12}	NaN	1.21178×10^{-12}	2.64199×10^{-8}	1.21178×10^{-12}
F20	2.36567×10^{-12}	2.36567×10^{-12}	2.36567×10^{-12}	2.36567×10^{-12}	2.36567×10^{-12}	3.26247×10^{-13}	2.36567×10^{-12}	1.37344×10^{-11}	2.36567×10^{-12}

5.1.2. Analysis of Experimental Results of CEC2014 and CEC2017 Combined Test Functions

The ability of the algorithm to find the global optimal solution is evaluated by the combined test functions in CEC2014 and CEC2017. The test results of MPSOGOA and the other nine comparison algorithms are shown in Table 7. As can be seen from Table 7, the improvement of MPSOGOA has achieved better optimization effects in all combined functions. In the test of function F21, MPSOGOA becomes the only one that converges to the global optimal solution successfully. In addition, in the tests of F23, F24, and F31, the MPSOGOA and GOAs successfully find the global optimal solution. However, by comparing the standard deviation, it can be found that MPSOGOA has higher stability in the search process and can find the global optimal solution more stably. For F22, F25, F26, F27, F29, F30, F34, and F35 functions, MPSOGOA has achieved significant improvement in both optimization accuracy and stability compared with GOA. This series of improvements not only enhances the robustness of the algorithm, but also further validates the advantages of MPSOGOA in solving complex optimization problems. In summary, MPSOGOA successfully improves the ability of global optimal solution search by combining the advantages of PSO and gazelle optimization. Whether faced with the challenge of a single function or a series of combined functions, MPSOGOA has demonstrated its superior optimization performance and stability.

Table 7. CEC2014 and CEC2017 combined test function results.

Function	Value	MPSOGOA	GOA	GWO	SCA	AOA	PSO	DE	Chimp	BBO	GJO
F21	Best	100	100.002	497303	2.8751×10^{6}	1.8327×10^{7}	706.164	305.288	8.0177×10^{6}	2420.75	406266
	Worst	100.013	100.072	1.7767×10^{7}	1.9090×10^{7}	5.8279×10^{8}	1.1233×10^{6}	924.812	1.6256×10^{7}	625,239	1.2559×10^{7}
	Average	100.004	100.017	6.0640×10^{6}	8.9227×10^{6}	1.4787×10^{8}	204,591	564.505	1.2709×10^{7}	58,141	6.0484×10^{6}
	SD	0.00290333	0.0167286	4.8059×10^{6}	4.0258×10^{6}	1.4225×10^{8}	262,795	166.633	1.9064×10^{6}	118,913	3.4408×10^{6}
	Median	100.003	100.011	4.3561×10^{6}	8.9623×10^{6}	8.8048×10^{7}	140,538	530.48	1.2823×10^{7}	16,120	6.3206×10^{6}
F22	Best	100.014	100.352	4954.71	4.0935×10^{8}	3.3875×10^{9}	121.639	100	1.1187×10^{8}	104.425	42,465.7
	Worst	101.712	109.656	2.4920×10^{8}	1.0862×10^{9}	1.8657×10^{10}	41,644.1	100.008	4.5520×10^{9}	3737.5	8.4987×10^{8}
	Average	100.253	101.87	1.0144×10^{7}	6.9655×10^{8}	1.0337×10^{10}	7004.88	100.002	1.1031×10^{9}	909.021	2.3983×10^{8}
	SD	0.32865	1.7876	4.5633×10^{7}	1.9790×10^{8}	4.5134×10^{09}	11,046.5	0.00185375	1.1161×10^{9}	985.875	2.2961×10^{8}
	Median	100.16	101.41	37981.7	7.1394×10^{8}	9.3369×10^{09}	2040.91	100.002	8.7509×10^{8}	536.839	3.2297×10^{8}
F23	Best	300	300	304.02	590.685	7784.51	300	300.002	865.755	300.003	369.827
	Worst	300	300	10060.8	4488.05	44,057.3	300	300.14	5496.47	300.394	11,775.7
	Average	300	300	2221.82	1464.07	19086.5	300	300.044	2668.99	300.075	3419.88
	SD	2.10829×10^{-6}	2.32747×10^{-5}	2162.58	933.659	6226.11	1.25015×10^{-10}	0.038889	929.853	0.0997502	3166.9
	Median	300	300	1738.23	1133.22	18232	300	300.028	2430.42	300.035	2529.64
F24	Best	400	400	406.856	420.009	605.459	401.883	400.001	437.39	400.036	402.817
	Worst	400.002	400.06	464.024	530.424	3059.65	407.88	400.005	866.152	406.017	517.397
	Average	400	400.012	415.454	446.743	1428.42	404.726	400.002	580.915	404.132	433.261
	SD	0.00039569	0.012884	16.0304	20.2286	618.579	0.875749	0.00090655	130.319	1.78863	26.7036
	Median	400	400.007	407.635	444.704	1315.07	404.746	400.002	523.902	404.847	421.237
F25	Best	504.727	506.666	504.029	528.916	551.155	503.98	520.522	540.112	504.975	512.722
	Worst	513.63	514.617	537.064	560.343	625.244	519.902	540.786	587.365	524.874	555.559
	Average	508.511	510.379	514.963	548.622	583.175	510.771	531.554	554.881	513.234	529.777
	SD	1.93091	2.04348	8.19723	6.57421	20.0004	4.03449	4.53236	9.20563	5.28014	11.9866
	Median	508.738	510.071	513.347	549.388	581.339	511.472	531.372	553.097	511.939	526.234
F26	Best	600.053	600.691	600.452	604.75	608.165	600	600.015	604.828	600.102	601.404
	Worst	600.557	603.544	604.933	609.084	612.301	602.197	606.581	610.065	605.684	606.633
	Average	600.238	602.438	601.716	606.656	610.676	600.363	603.293	607.317	602.333	603.773
	SD	0.137944	0.60068	0.950969	1.09467	1.01231	0.492687	2.18072	0.93655	1.52371	1.38629
	Median	600.202	602.562	601.605	606.452	610.915	600.235	603.032	607.242	602.21	603.802
F27	Best	600.029	600.136	600.031	611.913	625.002	600	600	614.988	600	600.128
	Worst	600.213	600.626	603.186	622.485	666.45	600	600.001	649.476	600.007	617.374
	Average	600.099	600.314	600.865	616.557	646.758	600	600	626.284	600.002	606.311
	SD	0.0439481	0.0968376	0.863563	3.1968	11.1953	4.82533×10^{-6}	0.00012652	9.09013	0.00180132	5.32735
	Median	600.091	600.321	600.513	615.99	646.768	600	600	624.155	600.001	604.569
F28	Best	717.354	715.188	711.123	744.22	789.468	706.599	734.649	745.94	714.339	727.013
	Worst	730.508	729.692	749.49	794.554	846.893	729.782	753.924	837.24	730.971	771.148
	Average	722.498	723.365	727.096	771.986	818.838	719.003	745.343	801.477	721.941	748.372
	SD	3.17343	3.7817	10.0467	9.96861	13.2701	6.20277	5.28398	19.2928	4.76201	11.2874
	Median	721.983	723.411	724.864	772.418	819.667	719.282	746.894	807.692	721.982	748.563
F29	Best	801.871	803.593	803.001	816.145	864.897	800	815.332	823.349	802.985	805.041
	Worst	806.832	809.639	821.893	850.156	922.149	804.975	827.947	873.689	816.914	854.547
	Average	804.63	806.501	809.096	839.185	887.82	802.487	822.194	840.304	807.495	824.501
	SD	1.0983	1.60518	4.80148	7.44689	10.8391	1.47229	3.32467	9.6011	3.66488	13.7031
	Median	804.763	806.404	807.964	839.885	886.478	801.99	821.908	838.181	806.467	820.065
F30	Best	802.303	803.97	804.998	820.51	831.099	802.985	824.307	826.267	802.985	815.053
	Worst	811.626	814.144	823.188	856.539	887.042	818.904	846.226	857.065	833.829	848.545
	Average	807.658	809.333	812.491	840.278	861.966	809.571	834.215	839.906	814.825	825.801
	SD	2.0394	2.31246	4.98893	8.43299	14.2366	3.83144	5.42961	9.01636	7.28028	9.38006
	Median	807.596	809.14	811.194	839.749	862.644	809.95	834.559	839.66	814.429	821.687
F31	Best	900	900.002	900.012	937.24	1062.16	900	900	969.749	900	900.473
	Worst	900.001	900.129	965.559	1076.54	1795.06	900	900	1798.09	900	1223.07
	Average	900	900.042	907.692	1013.15	1428.2	900	900	1368.72	900	968.069
	SD	0.00013829	0.0349609	16.5886	33.8893	206.925	5.58548×10^{-14}	6.18317×10^{-11}	210.66	0.00013770	74.1475
	Median	900	900.027	900.64	1018.3	1433.51	900	900	1330.54	900	962.495
F32	Best	1019.92	1050.82	1015.37	1686.93	1556.4	1006.89	1158.78	1357.15	1007.02	1234.96
	Worst	1156.87	1189.75	1781.65	2398.98	2429.74	1417.13	1733.54	2556.45	1572.39	1945.8
	Average	1093.57	1092.34	1285.75	2014.23	2015.77	1164.4	1355.84	2015.19	1205.3	1567.49
	SD	51.4649	38.6527	163.457	183.646	239.863	117.962	139.823	263.348	136.006	216.077
	Median	1089.8	1076.48	1265	1998.83	2014.74	1148.06	1328.51	2003.17	1190.88	1553.16
F33	Best	1149.86	1226.22	1123.75	1857.14	2183.58	1222.37	1758.82	1754.37	1332.32	1139.14
	Worst	1624.68	1744.55	1970.53	2813.92	3097.35	2116.45	2604.7	2814.13	2716.32	2373.31
	Average	1387.06	1470.59	1539.5	2401.94	2655.47	1566.41	2306.49	2378.16	1854.5	1747
	SD	118.75	128.246	158.502	219.785	234.239	256.108	218.937	240.691	316.273	265.919
	Median	1381.09	1473.4	1557.3	2440.76	2675.11	1548.76	2388.02	2379.04	1777.54	1712.93
F34	Best	1100.7	1101.92	1106.38	1139.93	1510.68	1100.09	1105.72	1152.88	1103.57	1104.14
	Worst	1103.91	1106.45	1245.36	1299.55	23,686.5	1112.66	1112.17	1454.55	1178.05	1410.05
	Average	1102.57	1103.77	1134.5	1195.36	6201.99	1105.26	1109.08	1297.52	1125.37	1167.14
	SD	0.784066	1.10189	33.7692	35.319	5397.03	3.23331	1.58061	103.312	18.4302	60.1217
	Median	1102.7	1103.88	1126.76	1188.5	4645.15	1105.07	1109.15	1320.93	1119.59	1148.68
F35	Best	1601.28	1601.73	1601.31	1602.7	1602.85	1601.18	1603.27	1602.34	1601.52	1601.45
	Worst	1602.5	1603.14	1603.52	1603.85	1604.29	1603.13	1603.74	1603.52	1603.44	1603.47
	Average	1602.12	1602.7	1602.56	1603.35	1603.7	1602.39	1603.48	1603.14	1602.73	1602.81
	SD	0.29735	0.334147	0.509288	0.259755	0.33964	0.52719	0.126328	0.243251	0.423091	0.410734
	Median	1602.16	1602.78	1602.54	1603.35	1603.73	1602.38	1603.44	1603.22	1602.74	1602.85

Compared to the GOA, MPSOGOA exhibits improved convergence accuracy and a strong ability to escape local optima. Additionally, it achieves smaller standard deviations, notably reducing the standard deviations in F21, F22, F24, and F31, suggesting that MPSOGOA significantly surpasses the GOA in terms of stability.

Table 8 shows the results of the Wilcoxon signed-rank test for 15 composite functions. The results show that there are significant differences between MPSOGOA and other algorithms on most test functions.

Table 8. Wilcoxon signed-rank test results of CEC2014 and CEC2017 combined test functions.

Function	GOA	GWO	SCA	AOA	PSO	DE	Chimp	BBO	GJO
F21	5.59991×10^{-7}	3.01986×10^{-11}	3.01986×10^{-11}	3.01986×10^{-11}	3.01986×10^{-11}	3.01986×10^{-11}	3.01986×10^{-11}	3.01986×10^{-11}	3.01986×10^{-11}
F22	7.38029×10^{-10}	3.01986×10^{-11}	3.01986×10^{-11}	3.01986×10^{-11}	3.01986×10^{-11}	3.01986×10^{-11}	3.01986×10^{-11}	3.01986×10^{-11}	3.01986×10^{-11}
F23	1.09367×10^{-10}	3.01986×10^{-11}	3.01986×10^{-11}	3.01986×10^{-11}	2.8502×10^{-11}	3.01986×10^{-11}	3.01986×10^{-11}	3.01986×10^{-11}	3.01986×10^{-11}
F24	1.77691×10^{-10}	3.01986×10^{-11}	3.01986×10^{-11}	3.01986×10^{-11}	3.01986×10^{-11}	3.82016×10^{-10}	3.01986×10^{-11}	3.01986×10^{-11}	3.01986×10^{-11}
F25	0.000654865	0.000200581	3.01986×10^{-11}	3.01986×10^{-11}	0.0169212	3.01986×10^{-11}	3.01986×10^{-11}	2.27802×10^{-5}	3.33839×10^{-11}
F26	3.01986×10^{-11}	4.50432×10^{-11}	3.01986×10^{-11}	3.01986×10^{-11}	0.923442	8.89099×10^{-10}	3.01986×10^{-11}	5.46175×10^{-9}	3.01986×10^{-11}
F27	8.15274×10^{-11}	1.74791×10^{-5}	3.01986×10^{-11}	3.01986×10^{-11}	1.53022×10^{-11}	3.01986×10^{-11}	3.01986×10^{-11}	3.01986×10^{-11}	7.38908×10^{-11}
F28	0.258051	0.0614519	3.01986×10^{-11}	3.01986×10^{-11}	0.0162848	3.01986×10^{-11}	3.01986×10^{-11}	0.589451	4.97517×10^{-11}
F29	1.24932×10^{-5}	6.2828×10^{-6}	3.01986×10^{-11}	3.01986×10^{-11}	1.25245×10^{-6}	3.01986×10^{-11}	3.01986×10^{-11}	0.000952074	1.09367×10^{-10}
F30	0.00508422	8.66343×10^{-5}	3.01986×10^{-11}	3.01986×10^{-11}	0.0405755	3.01986×10^{-11}	3.01986×10^{-11}	4.35308×10^{-5}	3.01986×10^{-11}
F31	3.01986×10^{-11}	3.01986×10^{-11}	3.01986×10^{-11}	3.01986×10^{-11}	7.57407×10^{-12}	3.01041×10^{-11}	3.01986×10^{-11}	0.0823572	3.01986×10^{-1}
F32	0.579294	2.02829×10^{-7}	3.01986×10^{-11}	3.01986×10^{-11}	0.0391671	3.01986×10^{-11}	3.01986×10^{-11}	0.00333861	3.01986×10^{-11}
F33	0.0206807	0.000124771	3.01986×10^{-11}	3.01986×10^{-11}	0.00728836	3.01986×10^{-11}	3.01986×10^{-11}	4.57257×10^{-9}	5.0922×10^{-8}
F34	5.97056×10^{-5}	3.01986×10^{-11}	3.01986×10^{-11}	3.01986×10^{-11}	4.35308×10^{-5}	3.01986×10^{-11}	3.01986×10^{-11}	3.33839×10^{-11}	3.01986×10^{-11}
F35	3.64589×10^{-8}	3.15727×10^{-5}	3.01986×10^{-11}	3.01986×10^{-11}	0.017649	3.01986×10^{-11}	6.06576×10^{-11}	6.01039×10^{-8}	7.11859×10^{-9}

The rankings of the Friedman test are given in Table 9. MPSOGOA first among the 10 algorithms, proving that MPSOGOA's optimization ability exceeds other algorithms. This shows that MPSOGOA has good optimization capabilities and can solve most optimization problems.

Table 9. Friedman ranking of CEC2014 and CEC2017 combination functions.

Algorithm	Friedman Mean Rank	General Mean Rank
MPSOGOA	1.7	1
GOA	3	3
GWO	5.13333	6
SCA	8	8
AOA	10	10
PSO	2.86667	2
DE	4.8	5
Chimp	8.66667	9
BBO	4.1	4
GJO	6.73333	7

5.1.3. Convergence Speed

Figure 6 compares the convergence curves of MPSOGOA with the original GOA and eight other optimization algorithms on the classical test functions. The behavior of optimization algorithms that converge to the optimal solution early in the optimization process can lead to the inability of the algorithm to find the final global optimal solution. It can be observed that MPSOGOA quickly converges to the optimal solution in most test functions without being constrained by local optima. The convergence curves of F1–F4 demonstrate the accelerated convergence speed of MPSOGOA. The early convergence to the optimal solution in F5, F9, F10, F11, F15, and F20 is attributed to the role of the chaotic strategy and population-wide perturbation in the initial iterations. The algorithm stalls in the later iterations of F7, and the individual experience of particles and population-wide perturbation play a role in the later iterations, enabling the algorithm to escape local optima and eventually find the global optimal solution. Compared to GOA, MPSOGOA significantly converges faster to the global optimal solution in F1–F7, F9–F13, and F15.

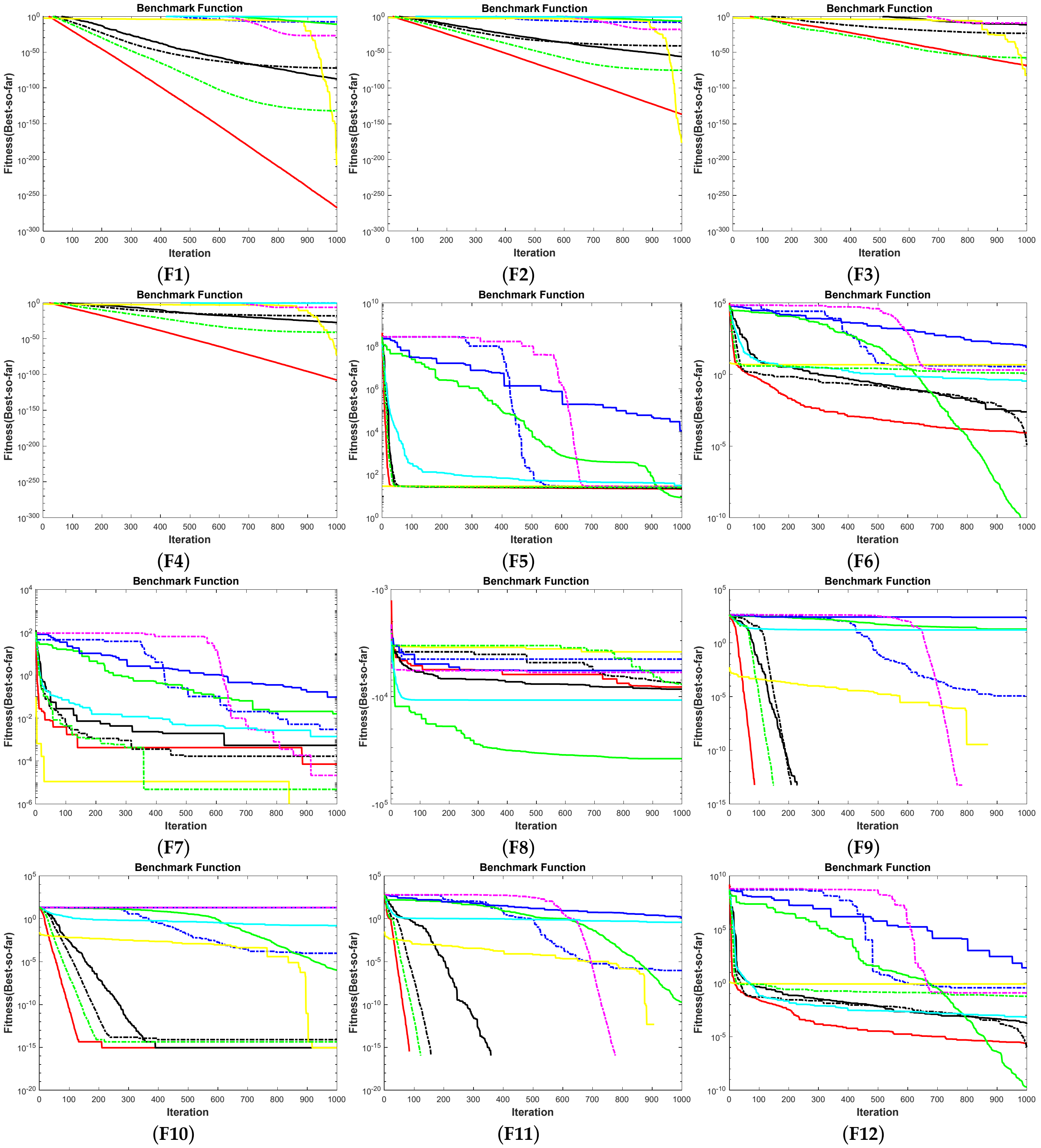

(F1) (F2) (F3)

(F4) (F5) (F6)

(F7) (F8) (F9)

(F10) (F11) (F12)

Figure 6. *Cont.*

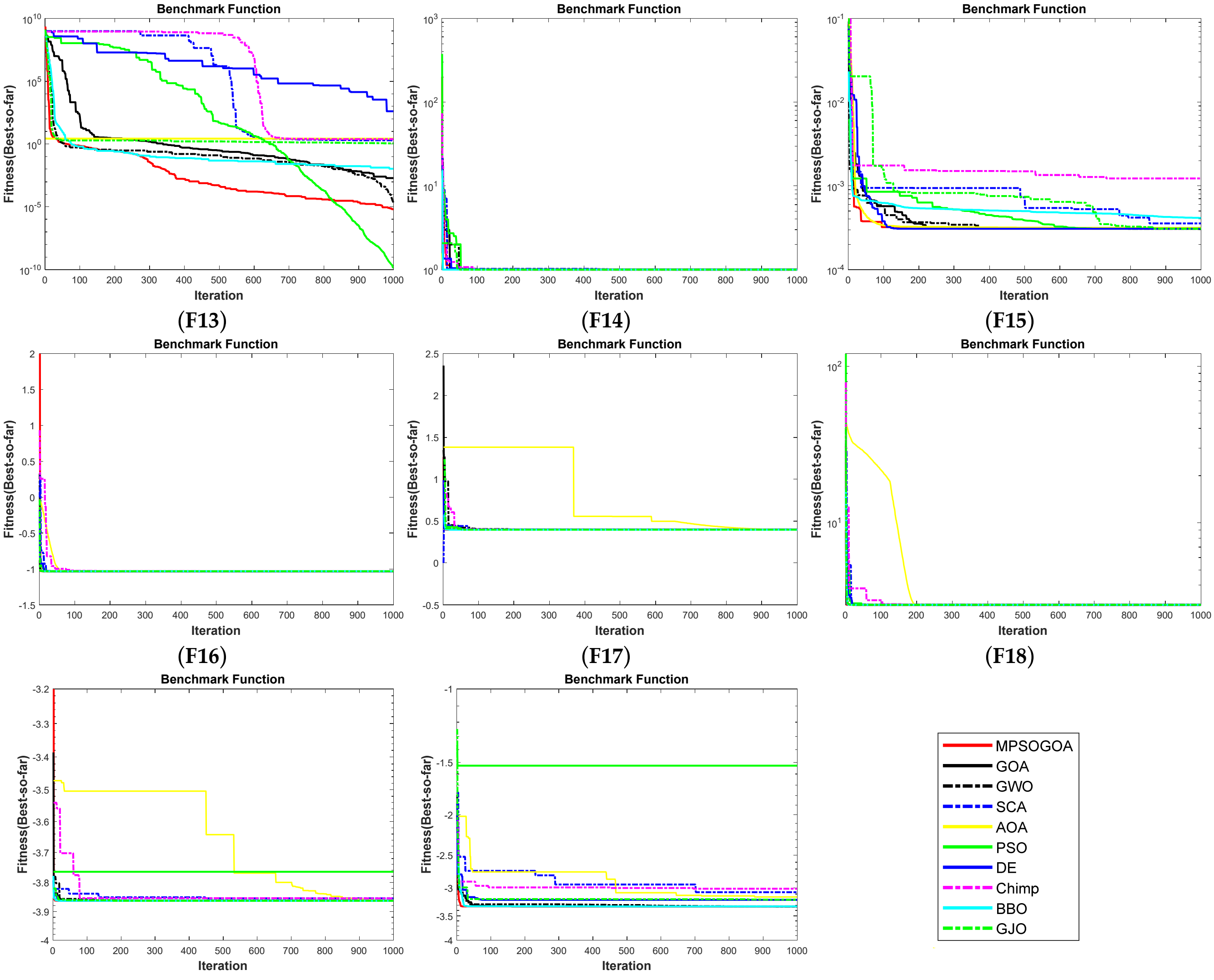

(F13) (F14) (F15)

(F16) (F17) (F18)

(F19) (F20)

Figure 6. CEC2005 test function convergence diagram.

Figure 7 shows the comparison of convergence curves of MPSOGOA, GOA, and eight other optimization algorithms in CEC2014 and CEC2017 combined test functions. Compared with other algorithms, MPSOGOA has an advantage in convergence speed. The convergence curve of MPSOGOA is always lower than the convergence curve of other algorithms, and the convergence curve drops significantly faster. The convergence rate of MPSOGOA on F21, F26, F27, F28, and F31 is obviously better than other algorithms. In the early stage of iteration, MPSOGOA's convergence ability is far superior to other algorithms, and it can quickly approach the optimal solution in a short time. This is because the algorithm adopts PLCM for population initialization in the initial stage, constructs the initial population with relatively uniform distribution, and improves the quality of the initial population, especially in the initial stage of functions F21 and F31, which have better fitness values than other algorithms. In addition, MPSOGOA shows stable and fast convergence on function F23 with small fluctuation due to the combination of population global perturbation strategy and particle swarm strategy. This further confirms MPSOGOA's significant advantages in terms of global convergence speed and optimization accuracy.

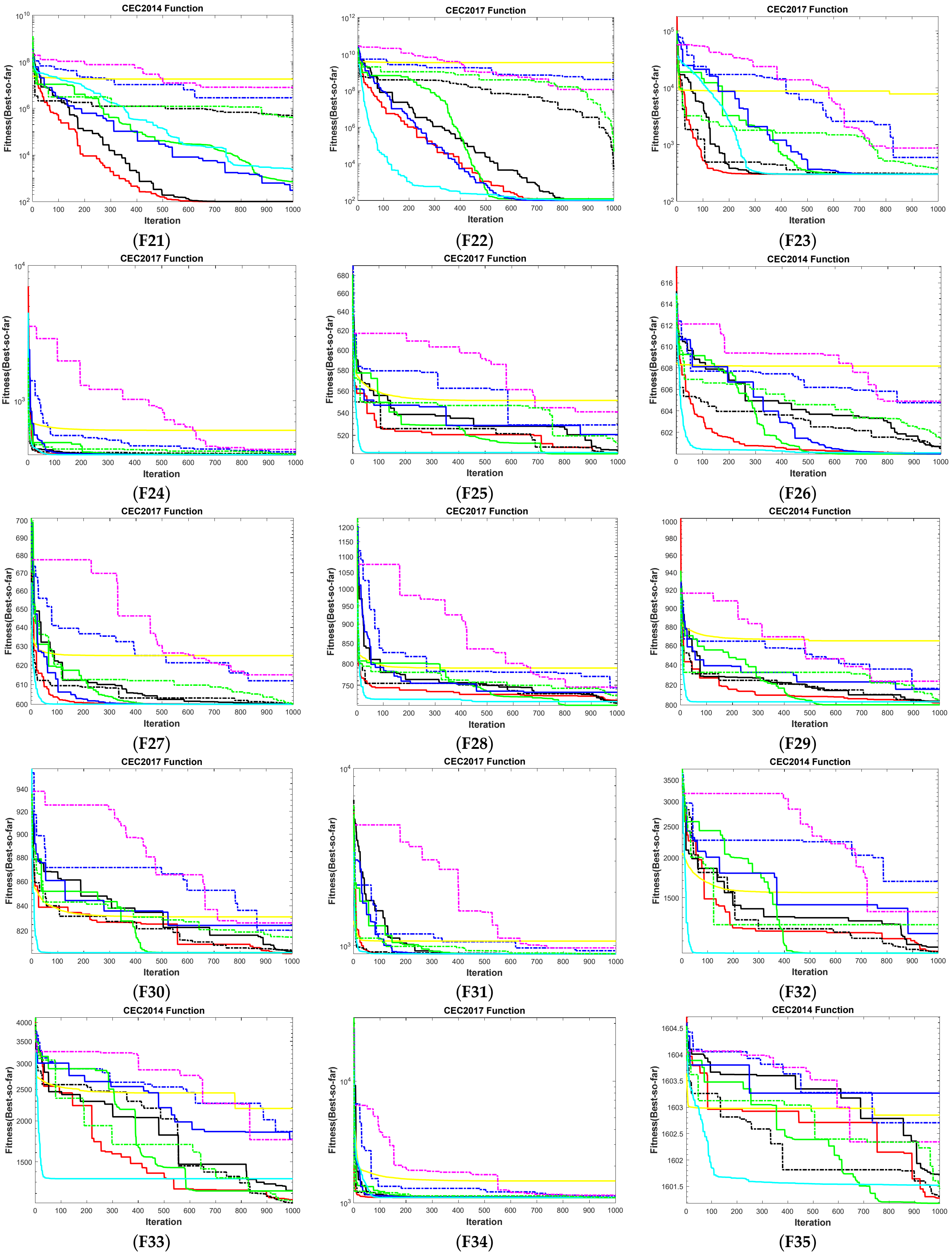

(F21) (F22) (F23)

(F24) (F25) (F26)

(F27) (F28) (F29)

(F30) (F31) (F32)

(F33) (F34) (F35)

Figure 7. Convergence diagram of CEC2014 and CEC2017 group and test functions.

After comprehensive analysis of MPSOGOA's optimization accuracy and convergence speed, the MPSOGOA has significantly improved both in terms of convergence speed and global optimization accuracy, and shows advantages in terms of stability. Compared with other algorithms, MPSOGOA has less fluctuation in results during multiple runs, meaning that its output results are more reliable and stable. The improved method is effective.

5.1.4. Ablation Experiment

Ablation experiments were conducted on MPSOGOA and GOA in order to comprehensively validate the effectiveness of the three proposed strategies during the optimization process. Three strategies were employed in this study to enhance the performance of GOA, leading to the following scenarios: the use of only the PWLC mapping strategy in the gazelle optimization algorithm (GOA1), the use of only population-wide disturbance in the gazelle optimization algorithm (GOA2), the use of only the PSO algorithm-integrated gazelle optimization algorithm (GOA3), the simultaneous use of PWLC mapping and population-wide disturbance strategies in the gazelle optimization algorithm (GOA4), the simultaneous use of PWLC mapping and PSO strategy-integrated gazelle optimization algorithm (GOA5), and the simultaneous use of population-wide disturbance and PSO strategy-integrated gazelle optimization algorithm (GOA6). The tests were based on classical test functions from Table 10 with a population size set at 50 and iteration count at 1000 in the experiments. Each algorithm was independently run 30 times, and calculations were performed for the optimal value, worst value, average value, standard deviation, and median.

It is evident that the convergence accuracy of the GOA1 algorithm from Table 10 and Figure 8, which incorporates only the PWLC mapping strategy, the GOA2 algorithm with only the population-wide disturbance strategy, and the GOA3 algorithm with only the strategy integrated with PSO, surpasses that of the standard GOA across 15 test functions. Furthermore, the convergence speed on these 15 test functions is also superior to that of the GOA. This indicates the efficacy of each strategy in enhancing the GOA. A comparative analysis between the optimization results of GOA1, GOA2, and GOA3 with GOA4, GOA5, and GOA6 reveals that the convergence accuracy achieved by the fusion of two improvement strategies is generally superior to that achieved using a single improvement strategy.

Simultaneously, the convergence speed is also enhanced, underscoring the synergistic and stable effectiveness of all improvement strategies. Their collective impact serves to improve the solving capability of MSPGOA. It can be also observed that the convergence accuracy of MPSOGOA from Table 10 and Figure 8, which integrate three improvement strategies, surpasses that of GOAs employing one or two improvement strategies. Notably, MPSOGOA exhibits the fastest convergence speed among the 15 test functions.

5.2. Engineering Problem Results

5.2.1. Welded Beam

Table 11 presents the experimental results of the welded beam design problem. The table includes the optimal solution obtained by MPSOGOA and the other nine optimization algorithms (GOA, GWO, SCA, AOA, PSO, DE, Chimp, BBO, and GJO) in the welded beam design problem, along with their corresponding optimal variables, worst value, mean, standard deviation, and median, as well as the values from the signed-rank test. It is evident from the table that the statistical results of all performance aspects of the proposed MPSOGOA in the welded beam design problem are optimal, indicating its strong optimization effectiveness in solving practical engineering applications and effectively reducing the cost of the welded beam design problem. The table indicates that MPSOGOA achieves the optimal cost value of 1.67022 for the welded beam design, with the corresponding optimal decision variables being steel bar length 0.198832, steel bar height 3.33737, steel bar thickness 9.19202, and weld thickness 0.198832. Compared to the original GOA, MPSOGOA exhibits a smaller standard deviation, signifying its superior stability. The results of the signed-rank test in the table indicate that the p-values for MPSOGOA and the other nine algorithms are all less than 0.05, indicating no statistical significance.

Table 10. Ablation experiment results based on CEC2005.

Function	Value	MPSOGOA	GOA1	GOA2	GOA3	GOA4	GOA5	GOA6	GOA
F1	Best	3.075×10^{-266}	2.152×10^{-133}	3.138×10^{-229}	4.569×10^{-177}	5.990×10^{-230}	1.352×10^{-150}	2.931×10^{-250}	1.070×10^{-83}
	Worst	1.420×10^{-213}	9.226×10^{-43}	1.819×10^{-176}	4.172×10^{-84}	8.633×10^{-182}	5.474×10^{-48}	1.106×10^{-193}	3.534×10^{-27}
	Average	4.734×10^{-215}	3.095×10^{-44}	6.063×10^{-178}	1.390×10^{-85}	3.15×10^{-183}	1.824×10^{-49}	3.690×10^{-195}	1.178×10^{-28}
	SD	0	1.684×10^{-43}	0	7.617×10^{-85}	0	9.995×10^{-49}	0	6.452×10^{-28}
	Median	4.110×10^{-256}	5.247×10^{-116}	7.028×10^{-215}	1.204×10^{-161}	1.009×10^{-221}	1.328×10^{-142}	8.663×10^{-236}	6.043×10^{-72}
F2	Best	3.097×10^{-137}	1.831×10^{-79}	2.573×10^{-119}	2.799×10^{-87}	7.213×10^{-119}	2.021×10^{-87}	1.374×10^{-127}	2.420×10^{-54}
	Worst	8.387×10^{-120}	6.225×10^{-34}	6.162×10^{-95}	1.217×10^{-34}	1.759×10^{-95}	2.160×10^{-37}	2.404×10^{-101}	3.423×10^{-15}
	Average	6.067×10^{-121}	2.610×10^{-35}	2.739×10^{-96}	4.078×10^{-36}	5.864×10^{-97}	7.203×10^{-39}	8.01×10^{-103}	1.141×10^{-16}
	SD	2.074×10^{-120}	1.163×10^{-34}	1.173×10^{-95}	2.222×10^{-35}	3.212×10^{-96}	3.94×10^{-38}	4.390×10^{-102}	6.251×10^{-16}
	Median	1.840×10^{-129}	2.150×10^{-75}	2.667×10^{-114}	4.423×10^{-80}	5.312×10^{-114}	1.104×10^{-80}	1.919×10^{-122}	1.904×10^{-49}
F3	Best	8.481×10^{-67}	1.966×10^{-32}	5.444×10^{-45}	2.346×10^{-23}	2.787×10^{-49}	8.461×10^{-25}	3.134×10^{-57}	2.760×10^{-14}
	Worst	6.098×10^{-43}	0.0063208	2.767×10^{-24}	5.087×10^{-5}	2.126×10^{-25}	0.0002043	7.001×10^{-40}	0.0948753
	Average	2.074×10^{-44}	0.0002166	9.225×10^{-26}	1.695×10^{-6}	7.0912×10^{-27}	8.407 × 10−06	2.635×10^{-41}	0.0050304
	SD	1.112×10^{-43}	0.0011531	5.052×10^{-25}	9.287×10^{-6}	3.882×10^{-26}	3.759×10^{-5}	1.281×10^{-40}	0.0197871
	Median	9.692×10^{-59}	4.349×10^{-9}	1.046×10^{-37}	2.756×10^{-16}	2.276×10^{-38}	1.822×10^{-16}	4.302×10^{-49}	1.543×10^{-8}
F4	Best	6.678×10^{-108}	7.057×10^{-33}	8.905×10^{-89}	6.233×10^{-40}	4.292×10^{-89}	8.042×10^{-40}	2.157×10^{-99}	1.138×10^{-26}
	Worst	1.712×10^{-89}	3.916×10^{-7}	3.050×10^{-67}	2.644×10^{-8}	1.110×10^{-68}	8.146×10^{-10}	3.119×10^{-76}	5.2×10^{-8}
	Average	5.718×10^{-91}	1.394×10^{-8}	1.017×10^{-68}	8.827×10^{-10}	3.702×10^{-70}	3.205×10^{-11}	1.039×10^{-77}	1.826×10^{-9}
	SD	3.127×10^{-90}	7.145×10^{-8}	5.569×10^{-68}	4.827×10^{-9}	2.027×10^{-69}	1.502×10^{-10}	5.695×10^{-77}	9.489×10^{-9}
	Median	7.126×10^{-103}	1.578×10^{-20}	1.885×10^{-84}	1.168×10^{-35}	7.537×10^{-83}	9.933×10^{-34}	1.822×10^{-91}	2.177×10^{-20}
F5	Best	20.8641	22.8216	22.6316	22.6042	21.9583	22.6008	21.4154	22.8925
	Worst	23.6918	24.2126	24.321	24.0658	23.7578	24.1712	23.692	24.5825
	Average	22.7685	23.7121	23.2368	23.3641	22.9723	23.4461	22.8734	23.7886
	SD	0.635053	0.34315	0.389083	0.334455	0.413717	0.400416	0.561724	0.393173
	Median	22.8497	23.807	23.2568	23.3893	23.0459	23.5037	22.9644	23.7909
F6	Best	4.644×10^{-5}	0.0003150	0.0005136	0.0006999	0.0002319	0.0001309	0.0007715	0.0012891
	Worst	0.0428836	0.0497734	0.0562091	0.0392158	0.0344983	0.0427188	0.0428622	0.0485372
	Average	0.0129548	0.0156648	0.0126048	0.0105064	0.0114111	0.0112348	0.0104577	0.0180974
	SD	0.0113952	0.0131013	0.0117002	0.0099258	0.0085911	0.0109503	0.0100127	0.0119936
	Median	0.0095370	0.0129409	0.0095088	0.0069833	0.0093544	0.0095399	0.0076343	0.0182215
F7	Best	7.929×10^{-5}	0.000251	0.0002996	0.0001754	0.0001650	0.0002388	0.0001523	0.0005179
	Worst	0.0024373	0.0038045	0.0026464	0.0049646	0.0027973	0.0044172	0.0026499	0.0042818
	Average	0.0006266	0.0013592	0.0010830	0.0010165	0.0011226	0.0008795	0.0008772	0.0014611
	SD	0.0005003	0.0008120	0.0005875	0.0011025	0.0006332	0.0008333	0.0005545	0.0008009
	Median	0.0004800	0.0012386	0.0009866	0.0005666	0.0010134	0.0005796	0.0008353	0.0013893
F8	Best	−8146.04	−8365.17	−8564.12	−8148.34	−8264.39	−8093.99	−8737.25	−8132.17
	Worst	−6929.54	−7210.73	−7268.81	−6990.89	−7101.98	−6783.8	−7018.35	−7031.04
	Average	−7447.88	−7632.9	−7775.89	−7504.24	−7543.32	−7505.6	−7812.09	−7618.5
	SD	308.101	269.635	361.109	228.649	255.94	316.665	386.591	321.743
	Median	−7483.99	−7602.55	−7725.42	−7490.31	−7497.32	−7591.64	−7731.38	−7690.26
F9	Best	0	0	0	0	0	0	0	0
	Worst	0	0	0	0	0	0	0	0
	Average	0	0	0	0	0	0	0	0
	SD	0	0	0	0	0	0	0	0
	Median	0	0	0	0	0	0	0	0
F10	Best	8.881×10^{-16}	8.881×10^{-16}	4.440×10^{-15}	8.881×10^{-16}	8.881×10^{-16}	4.440×10^{-15}	8.881×10^{-16}	8.881×10^{-16}
	Worst	4.440×10^{-15}	9.325×10^{-14}	4.440×10^{-15}	4.440×10^{-15}	4.440×10^{-15}	4.440×10^{-15}	4.440×10^{-15}	2.930×10^{-14}
	Average	4.322×10^{-15}	5.033×10^{-15}	4.440×10^{-15}	3.967×10^{-15}	4.322×10^{-15}	4.440×10^{-15}	4.322×10^{-15}	3.730×10^{-15}
	SD	6.486×10^{-16}	1.674×10^{-14}	0	1.228×10^{-15}	6.486×10^{-16}	0	6.486×10^{-16}	5.144×10^{-15}
	Median	4.440×10^{-15}	8.881×10^{-16}	4.440×10^{-15}	4.440×10^{-15}	4.440×10^{-15}	4.440×10^{-15}	4.440×10^{-15}	4.440×10^{-15}
F11	Best	0	0	0	0	0	0	0	0
	Worst	0	0	0	0	0	0	0	0
	Average	0	0	0	0	0	0	0	0
	SD	0	0	0	0	0	0	0	0
	Median	0	0	0	0	0	0	0	0
F12	Best	2.961×10^{-6}	4.071×10^{-5}	3.114×10^{-5}	9.267×10^{-6}	6.116×10^{-5}	4.519×10^{-5}	8.489×10^{-6}	0.0001418
	Worst	0.0009958	0.0009989	0.0008660	0.0012403	0.0013423	0.0010939	0.0018899	0.0026304
	Average	0.0003507	0.0003680	0.0002844	0.0003891	0.0003573	0.0004416	0.0003297	0.0007276
	SD	0.0002954	0.0002487	0.0002238	0.0003047	0.0002627	0.0003104	0.0004030	0.0005522
	Median	0.0002536	0.0003468	0.0002312	0.0003582	0.0003202	0.0004877	0.0001838	0.0005805
F13	Best	5.369×10^{-5}	0.0001331	0.002688	0.0017903	0.0007865	0.0012620	0.0018526	0.0030045
	Worst	0.153973	0.058177	0.0942476	0.0650685	0.0788267	0.0381157	0.114282	0.0634467
	Average	0.049772	0.0099884	0.0244842	0.015226	0.0273083	0.0144915	0.0266147	0.0213521
	SD	0.038678	0.012237	0.0213996	0.0149223	0.0229325	0.0110837	0.0258222	0.015971
	Median	0.036302	0.0063070	0.0205127	0.0114016	0.0209073	0.0102529	0.0186282	0.0188452
F14	Best	0.998004	0.998004	0.998004	0.998004	0.998004	0.998004	0.998004	0.998004
	Worst	0.998004	0.998004	0.998004	0.998004	0.998004	0.998004	0.998004	0.998004
	Average	0.998004	0.998004	0.998004	0.998004	0.998004	0.998004	0.998004	0.998004
	SD	0	0	5.831×10^{-17}	7.141×10^{-17}	5.831×10^{-17}	1.009×10^{-16}	7.141×10^{-17}	1.090×10^{-16}
	Median	0.998004	0.998004	0.998004	0.998004	0.998004	0.998004	0.998004	0.998004
F15	Best	0.0003074	0.0003074	0.0003074	0.0003074	0.0003074	0.00030748	0.0003074	0.0003074
	Worst	0.0003074	0.0003074	0.0003074	0.0003074	0.0003074	0.00030748	0.0003074	0.0003074
	Average	0.0003074	0.0003074	0.0003074	0.0003074	0.0003074	0.00030748	0.0003074	0.0003074
	SD	7.778×10^{-14}	6.976×10^{-13}	3.604×10^{-13}	4.829×10^{-13}	7.947×10^{-13}	9.449×10^{-13}	3.945×10^{-12}	5.754×10^{-13}
	Median	0.0003074	0.0003074	0.0003074	0.0003074	0.0003074	0.00030748	0.0003074	0.0003074

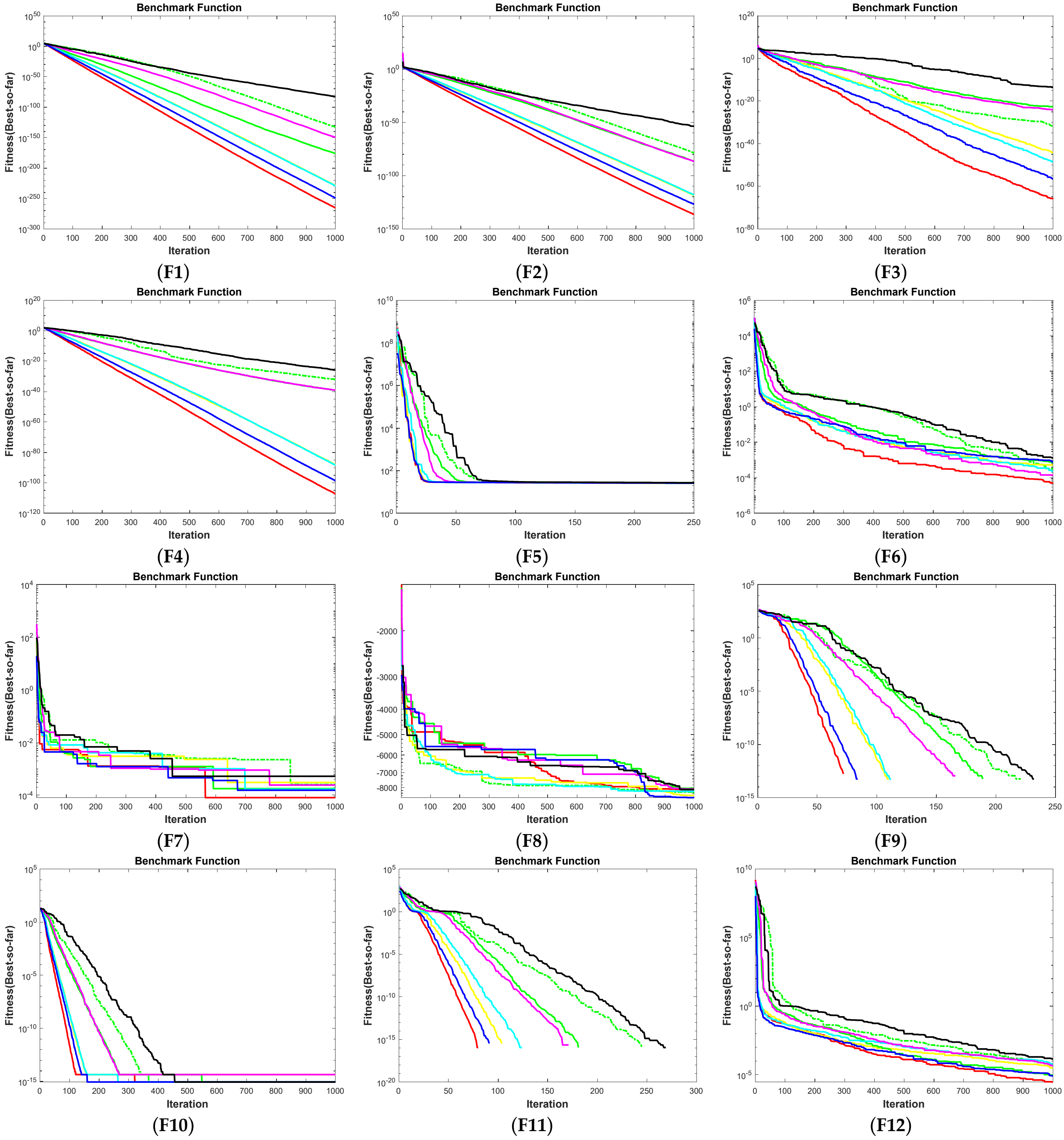

(F1)

(F2)

(F3)

(F4)

(F5)

(F6)

(F7)

(F8)

(F9)

(F10)

(F11)

(F12)

Figure 8. *Cont.*

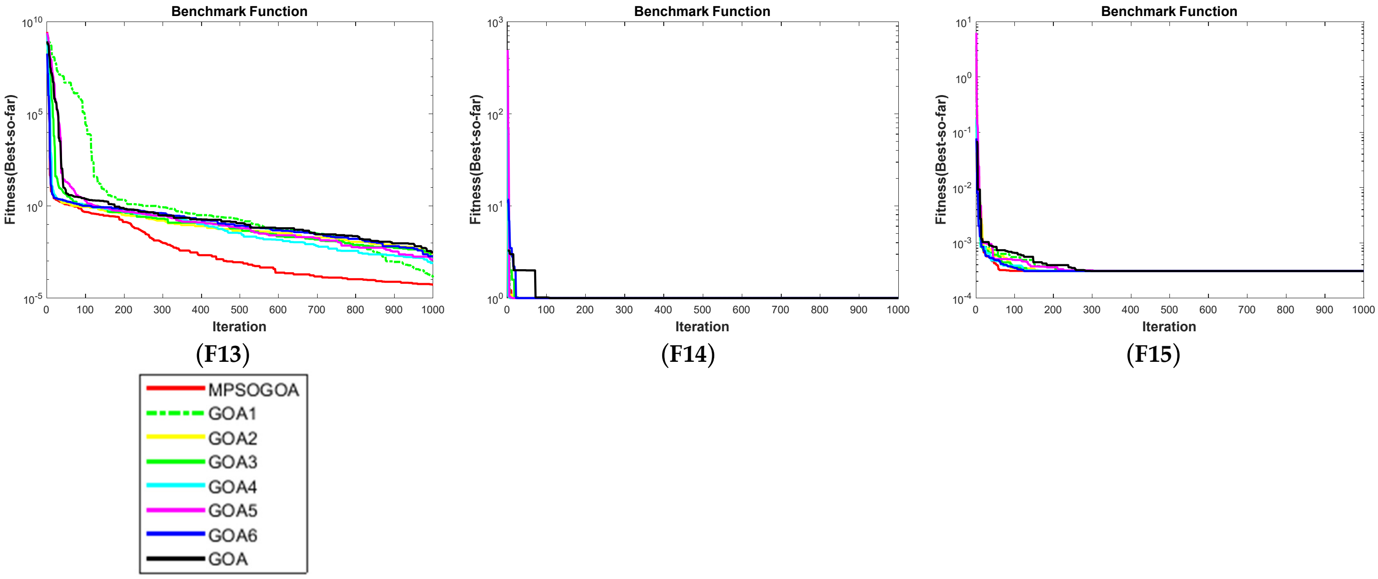

(F13) (F14) (F15)

Figure 8. Convergence results of ablation experiments based on CEC2005.

Table 11. Experimental results of WBD.

	h	l	t	b	Best	Worst	Average	SD	Median	*p*
MPSOGOA	0.198832	3.33737	9.19202	0.198832	1.67022	1.67022	1.67022	6.9276×10^{-7}	1.67022	N/A
GOA	0.198832	3.33736	9.19203	0.198832	1.67022	1.67023	1.67022	2.7146×10^{-6}	1.67022	4.117×10^{-6}
GWO	0.198676	3.34055	9.19251	0.19886	1.6707	1.67602	1.67224	0.0013803	1.67173	3.019×10^{-11}
SCA	0.189317	3.50989	9.36715	0.198795	1.70764	1.8522	1.79678	0.0335841	1.79892	3.019×10^{-11}
AOA	0.188049	3.7992	10	0.196186	1.82839	2.68791	2.34035	0.177038	2.36669	3.019×10^{-11}
PSO	0.169229	4.89949	9.14451	0.27382	2.43173	7.48264	5.06402	1.45427	5.01009	3.019×10^{-11}
DE	0.198832	3.33737	9.19202	0.198832	1.67022	1.67022	1.67022	1.7000×10^{-16}	1.67022	1.665×10^{-11}
Chimp	0.196437	3.40766	9.16569	0.202305	1.69817	1.7957	1.75433	0.0222802	1.75877	3.019×10^{-11}
BBO	0.25149	2.80336	8.1706	0.251664	1.85816	2.72723	2.1878	0.212509	2.19146	3.019×10^{-11}
GJO	0.198812	3.33722	9.1983	0.198841	1.67128	1.69453	1.6757	0.00463749	1.67429	3.019×10^{-11}

Figure 9 shows the convergence curves of each algorithm on the welded beam design problem. These algorithms can quickly converge to the optimal solution.

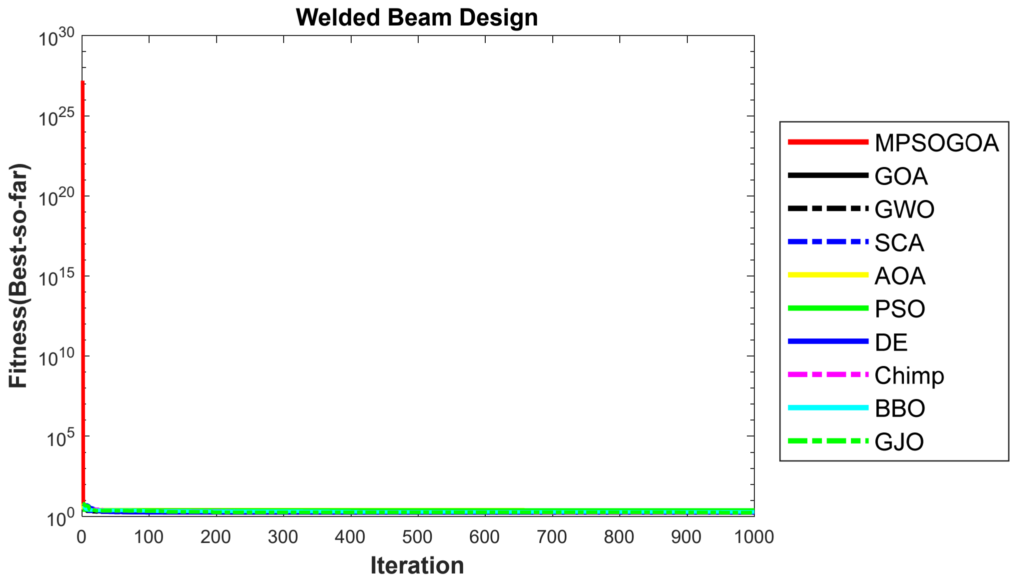

Figure 9. Convergence curve of WBD.

5.2.2. Compression Spring Design

Table 12 presents the experimental results for the compression spring design problem. The table includes the optimal solution obtained by MPSOGOA and the other nine optimization algorithms in the compression spring design problem, along with their corresponding optimal variables, worst value, mean, standard deviation, and median, as well as the values from the signed-rank test. It is evident from the table that MPSOGOA achieves the optimal cost value of 0.0126652 for the compression spring design, with the corresponding optimal decision variables being wire diameter 0.0516905, mean coil diameter 0.356752, and the number of effective coils in the spring 11.287. MPSOGOA and DE achieve the same optimal cost value in the compression spring design problem. Furthermore, when compared to the original GOA, MPSOGOA outperforms GOA in all statistical data aspects. The results of the signed-rank test in the table indicate that the *p*-values for MPSOGOA and the other nine algorithms are all less than 0.05, indicating no statistical significance.

Table 12. Experimental results of CSD.

	D	D	P	Best	Worst	Average	SD	Median	*p*
MPSOGOA	0.0516905	0.356752	11.287	0.0126652	0.0126655	0.0126653	5.92315×10^{-8}	0.0126653	N/A
GOA	0.0516822	0.356551	11.2987	0.0126653	0.0126658	0.0126654	1.14583×10^{-7}	0.0126654	0.000300589
GWO	0.0514958	0.352024	11.5769	0.0126741	0.0128559	0.0127191	3.08647×10^{-5}	0.0127213	3.01986×10^{-11}
SCA	0.0523236	0.370375	10.6095	0.012786	0.0132059	0.012966	0.000128481	0.0129485	3.01986×10^{-11}
AOA	0.05	0.310434	15	0.0131934	0.0305824	0.0141362	0.00367212	0.0131974	3.0123×10^{-11}
PSO	0.073141	0.76922	5.52228	0.0309544	8.64748×10^{9}	1.1754×10^{9}	2.05791×10^{9}	1.51764×10^{8}	3.01986×10^{-11}
DE	0.0516891	0.356718	11.289	0.0126652	0.0126652	0.0126652	2.69513×10^{-18}	0.0126652	1.5476×10^{-11}
Chimp	0.05	0.317316	14.0439	0.0127274	0.014333	0.0129773	0.000365126	0.0128398	3.01986×10^{-11}
BBO	0.0550947	0.444316	7.54043	0.012867	0.0178452	0.015147	0.00166555	0.0147453	3.01986×10^{-11}
GJO	0.0512038	0.345014	12.0291	0.0126903	0.0129066	0.0127409	4.6908×10^{-5}	0.0127318	3.01986×10^{-11}

Figure 10 shows the convergence curves of each algorithm on the welded beam design problem. Except for the PSO and Chimp algorithms, other algorithms can quickly converge to the optimal solution.

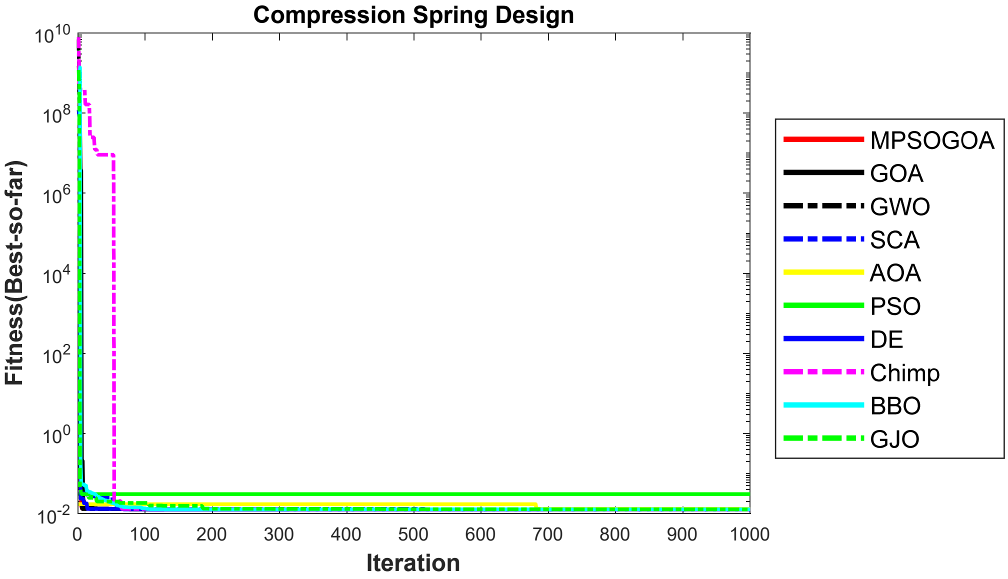

Figure 10. Convergence curve of CSD.

5.2.3. Pressure Vessel Design

Table 13 presents the experimental results for the pressure vessel design problem. The table includes the optimal solution obtained by MPSOGOA and the other nine optimization algorithms in the pressure vessel design problem, along with their corresponding optimal variables, worst value, mean, standard deviation, and median, as well as the values from the signed-rank test. It is evident from the table that the statistical results of all performance aspects of the proposed MPSOGOA in the pressure vessel design problem are optimal, indicating its strong optimization effectiveness in solving practical engineering applications and effectively reducing the cost of the pressure vessel design problem. From the table, it can be seen that MPSOGOA achieves the optimal cost value of 5885.33 for the pressure vessel design, with the corresponding optimal decision variables being pressure vessel thickness 0.778168, head thickness 0.384649, internal vessel radius 40.3196, and vessel head length 200. Compared to the original GOA, MPSOGOA exhibits significant improvement in terms of standard deviation, suggesting its superior stability in the process of seeking the optimal solution. The results of the signed-rank test in the table indicate that the *p*-values for MPSOGOA and the other nine algorithms are all less than 0.05, indicating no statistical significance.

Table 13. Experimental results of PVD.

	Ts	Th	R	L	Best	Worst	Average	SD	Median	*p*
MPSOGOA	0.778168	0.384649	40.3196	200	5885.33	5885.33	5885.33	0.0003421	5885.33	N/A
GOA	0.778168	0.384649	40.3196	200	5885.33	5885.34	5885.33	0.002140	5885.33	6.526×10^{-7}
GWO	0.778555	0.38478	40.3205	200	5888.65	6578.33	5937.79	135.014	5897.34	3.019×10^{-11}
SCA	0.90912	0.446679	46.4753	130.01	6236.74	8485.17	6854.85	559.787	6671.16	3.019×10^{-11}
AOA	0.906507	0.552833	41.7535	192.458	7429.05	30,021	12,804.8	5522.99	10978.9	3.019×10^{-11}
PSO	2.59675	11.605	68.0305	178.337	128,019	1.13904×10^{6}	484,168	275,483	383,206	3.019×10^{-11}
DE	0.778168	0.384649	40.3196	200	5885.33	5885.33	5885.33	2.775×10^{-12}	5885.33	1.211×10^{-12}
Chimp	0.842162	0.45967	40.7929	200	6659.64	8041.96	7655.43	285.916	7718.16	3.019×10^{-11}
BBO	0.817676	0.404177	42.3666	173.346	5956.45	7265.37	6477	353	6515.18	3.019×10^{-11}
GJO	0.778939	0.386412	40.3355	199.897	5896.41	7308.78	6198.12	462.634	5955.64	3.019×10^{-11}

Figure 11 shows the convergence curves of each algorithm on the pressure vessel design problem. MPSOGOA, GOA, GWO, SCA, DE, Chimp, and GJO are all able to quickly converge to the optimal solution. AOA falls into a local optimum and eventually escapes from the local optimum, and optimally converges to the optimal value.

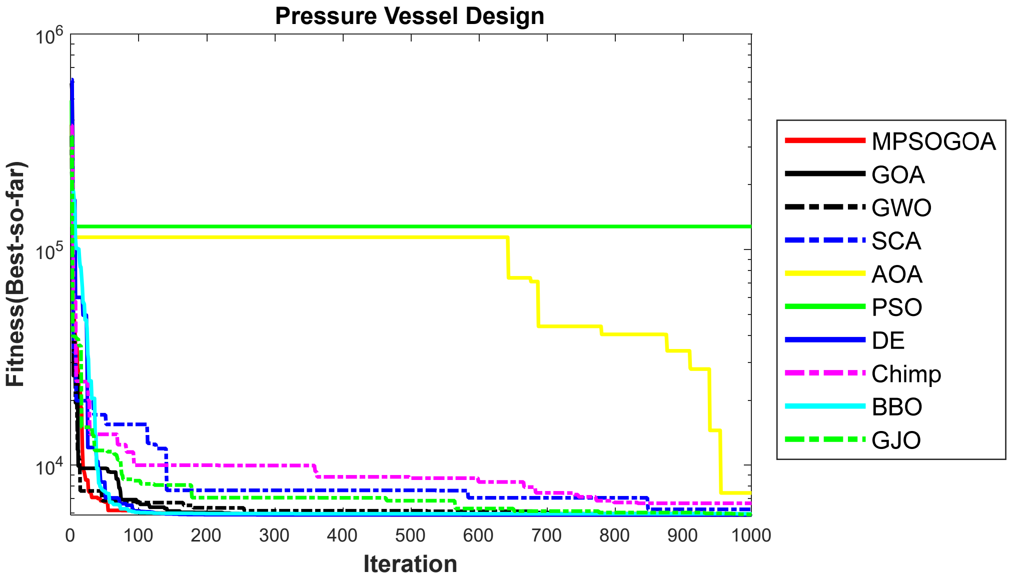

Figure 11. Convergence curve of PVD.

6. Conclusions

In this paper, we present an enhanced version of the MPSOGOA, incorporating a chaotic strategy to refine the quality of the initial population. A population-wide perturbation is strategically applied to augment the convergence speed and precision of the algorithm. Furthermore, through synergistic integration with PSO, emphasis is placed on leveraging individual experiences within the optimization process, culminating in a comprehensive enhancement of algorithmic performance. MPSOGOA demonstrates promising outcomes across a suite of 35 test functions and 4 engineering design challenges. Notably, in a majority of the test functions, MPSOGOA consistently identifies optimal solutions, displaying diminished standard deviations compared to the original GOA. This signifies a marked improvement in stability when contrasted with GOA. Additionally, in the Friedman test, MPSOGOA attains the foremost position among all comparative algorithms. Across the spectrum of four engineering design problems, the performance metrics of MPSOGOA surpass those of esteemed optimization algorithms including GOA, GWO, SCA, AOA, PSO, DE, Chimp, BBO, and GJO. To summarize, based on the comparative analysis of algorithms in both test functions and engineering designs, MPSOGOA emerges as a superior choice for addressing optimization challenges.

Author Contributions: Conceptualization, S.Q., H.Z., W.S. and J.Y.; methodology, J.Y. and J.W.; validation, S.Q., H.Z. and J.W.; formal analysis, J.Y.; investigation, J.Y.; resources, J.W.; data curation, H.Z.; writing—original draft preparation, S.Q. and H.Z.; writing—review and editing, J.Y. and J.W.; supervision, H.Z. All authors have read and agreed to the published version of the manuscript.

Funding: This research received no external funding.

Data Availability Statement: Data are contained within the article.

Conflicts of Interest: The authors declare no conflicts of interest.

References

1. Aditya, N.; Mahapatra, S.S. Switching from exploration to exploitation in gravitational search algorithm based on diversity with Chaos. *Inf. Sci.* **2023**, *635*, 298–327. [CrossRef]
2. Gonzalez-Ayala, P.; Alejo-Reyes, A.; Cuevas, E.; Mendoza, A. A Modified Simulated Annealing (MSA) Algorithm to Solve the Supplier Selection and Order Quantity Allocation Problem with Non-Linear Freight Rates. *Axioms* **2023**, *12*, 459. [CrossRef]
3. Zheng, W.M.; Liu, N.; Chai, Q.W.; Liu, Y. Application of improved black hole algorithm in prolonging the lifetime of wireless sensor network. *Complex Intell. Syst.* **2023**, *9*, 5817–5829. [CrossRef]
4. Mansuwan, K.; Jirapong, P.; Thararak, P. Optimal battery energy storage planning and control strategy for grid modernization using improved genetic algorithm. *Energy Rep.* **2023**, *9*, 236–241. [CrossRef]
5. Wei, L.; Zhang, Q.; Yang, B. Improved Biogeography-Based Optimization Algorithm Based on Hybrid Migration and Dual-Mode Mutation Strategy. *Fractal Fract.* **2022**, *6*, 597. [CrossRef]
6. Şahman, M.A.; Korkmaz, S. Discrete artificial algae algorithm for solving job-shop scheduling problems. *Knowl.-Based Syst.* **2022**, *256*, 109711. [CrossRef]
7. Salimon, S.A.; Adebayo, I.G.; Adepoju, G.A.; Adewuyi, O.B. Optimal Allocation of Distribution Static Synchronous Compensators in Distribution Networks Considering Various Load Models Using the Black Widow Optimization Algorithm. *Sustainability* **2023**, *15*, 15623. [CrossRef]
8. Umam, M.S.; Mustafid, M.; Suryono, S. A hybrid genetic algorithm and tabu search for minimizing makespan in flow shop scheduling problem. *J. King Saud Univ. -Comput. Inf. Sci.* **2022**, *34*, 7459–7467. [CrossRef]
9. János, M.M.; Artúr, S.; Gyula, G. Environmental and economic multi-objective optimization of a household level hybrid renewable energy system by genetic algorithm. *Appl. Energy* **2020**, *269*, 115058.
10. Lodewijks, G.; Cao, Y.; Zhao, N.; Zhang, H. Reducing CO_2 emissions of an airport baggage handling transport system using a particle swarm optimization algorithm. *IEEE Access* **2021**, *9*, 121894–121905. [CrossRef]
11. Abualigah, L.; Alkhrabsheh, M. Amended hybrid multi-verse optimizer with genetic algorithm for solving task scheduling problem in cloud computing. *J. Supercomput.* **2021**, *78*, 740–765. [CrossRef]
12. Hussain, B.; Khan, A.; Javaid, N.; Hasan, Q.U.; AMalik, S.; Ahmad, O.; Dar, A.H.; Kazmi, A. A WeightedSum PSO Algorithm for HEMS A New Approach for the Design and Diversified Performance Analysis. *Electronics* **2019**, *8*, 180. [CrossRef]
13. Paul, K.; Hati, D. A novel hybrid Harris hawk optimization and sine cosine algorithm based home energy management system for residential buildings. *Build. Serv. Eng. Res. Technol.* **2023**, *44*, 459–480. [CrossRef]
14. Jiang, C.; Yang, S.; Nie, P.; Xiang, X. Multi-objective structural profile optimization of ships based on improved Artificial Bee Colony Algorithm and structural component library. *Ocean. Eng.* **2023**, *283*, 115124. [CrossRef]
15. Abd Elaziz, M.; Dahou, A.; Mabrouk, A.; El-Sappagh, S.; Aseeri, A.O. An efficient artificial rabbits optimization based on mutation strategy for skin cancer prediction. *Comput. Biol. Med.* **2023**, *163*, 107154. [CrossRef] [PubMed]
16. Bishla, S.; Khosla, A. Enhanced chimp optimized self-tuned FOPR controller for battery scheduling using Grid and Solar PV Sources. *J. Energy Storage* **2023**, *66*, 107403. [CrossRef]
17. Percin, H.B.; Caliskan, A. Whale optimization algorithm based MPPT control of a fuel cell system. *Int. J. Hydrogen Energy* **2023**, *48*, 23230–23241. [CrossRef]
18. Jagadish Kumar, N.; Balasubramanian, C. Cost-efficient resource scheduling in cloud for big data processing using metaheuristic search black widow optimization (MS-BWO) algorithm. *J. Intell. Fuzzy Syst.* **2023**, *44*, 4397–4417. [CrossRef]

19. Zeng, C.; Qin, T.; Tan, W.; Lin, C.; Zhu, Z.; Yang, J.; Yuan, S. Coverage Optimization of Heterogeneous Wireless Sensor Network Based on Improved Wild Horse Optimizer. *Biomimetics* **2023**, *8*, 70. [CrossRef]
20. Chhabra, A.; Hussien, A.G.; Hashim, F.A. Improved bald eagle search algorithm for global optimization and feature selection. *Alex. Eng. J.* **2023**, *68*, 141–180. [CrossRef]
21. Liu, Y.; Sun, J.; Shang, Y.; Zhang, X.; Ren, S.; Wang, D. A novel remaining useful life prediction method for lithium-ion battery based on long short-term memory network optimized by improved sparrow search algorithm. *J. Energy Storage* **2023**, *61*, 106645. [CrossRef]
22. Xu, M.; Song, Q.; Xi, M.; Zhou, Z. Binary arithmetic optimization algorithm for feature selection. *Soft Comput.* **2023**, *27*, 11395–11429. [CrossRef] [PubMed]
23. Chen, M.; Huo, J.; Duan, Y. A hybrid biogeography-based optimization algorithm for three-dimensional bin size designing and packing problem. *Comput. Ind. Eng.* **2023**, *180*, 109239. [CrossRef]
24. Long, Y.; Liu, S.; Qiu, D.; Li, C.; Guo, X.; Shi, B.; AbouOmar, M.S. Local Path Planning with Multiple Constraints for USV Based on Improved Bacterial Foraging Optimization Algorithm. *J. Mar. Sci. Eng.* **2023**, *11*, 489. [CrossRef]
25. Zou, D.; Li, M.; Ouyang, H. A MOEA/D approach using two crossover strategies for the optimal dispatches of the combined cooling, heating, and power systems. *Appl. Energy* **2023**, *347*, 121498. [CrossRef]
26. Ramachandran, M.; Mirjalili, S.; Nazari-Heris, M.; Parvathysankar, D.S.; Sundaram, A.; Gnanakkan, C.A.R.C. A hybrid grasshopper optimization algorithm and harris hawks optimizer for combined heat and power economic dispatch problem. *Eng. Appl. Artif. Intell.* **2022**, *111*, 104753. [CrossRef]
27. Hamza, M.A.; Alshahrani, H.M.; Dhahbi, S.; Nour, M.K.; Al Duhayyim, M.; El Din, E.M.; Yaseen, I.; Motwakel, A. Differential Evolution with Arithmetic Optimization Algorithm Enabled Multi-Hop Routing Protocol. *Comput. Syst. Sci. Eng.* **2023**, *45*, 1759–1773. [CrossRef]
28. Pashaei, E.; Pashaei, E. Hybrid binary arithmetic optimization algorithm with simulated annealing for feature selection in high-dimensional biomedical data. *J. Supercomput.* **2022**, *78*, 15598–15637. [CrossRef]
29. Bhowmik, S.; Acharyya, S. Image encryption approach using improved chaotic system incorporated with differential evolution and genetic algorithm. *J. Inf. Secur. Appl.* **2023**, *72*, 103391. [CrossRef]
30. Panahizadeh, V.; Hamidi, E.; Daneshpayeh, S.; Saeifar, H. Optimization of impact strength and elastic modulus of polyamide-based nanocomposites: Using particle swarm optimization method. *J. Elastomers Plast.* **2024**, *56*, 244–261. [CrossRef]
31. Kim, K.H.; Jung, Y.H.; Shin, Y.J.; Shin, J.H. Optimizing the drainage system of subsea tunnels using the PSO algorithm. *Mar. Georesources Geotechnol.* **2024**, *42*, 266–278. [CrossRef]
32. Pal, K.; Verma, K.; Gandotra, R. Optimal location of FACTS devices with EVCS in power system network using PSO. *e-Prime—Adv. Electr. Eng. Electron. Energy* **2024**, *7*, 100482. [CrossRef]
33. Kang, Z.; Duan, R.; Zheng, Z.; Xiao, X.; Shen, C.; Hu, C.; Tang, S.; Qin, W. Grid aided combined heat and power generation system for rural village in north China plain using improved PSO algorithm. *J. Clean. Prod.* **2024**, *435*, 140461. [CrossRef]
34. Sirisumrannukul, S.; Intaraumnauy, T.; Piamvilai, N. Optimal control of cooling management system for energy conservation in smart home with ANNs-PSO data analytics microservice platform. *Heliyon* **2024**, *10*, e26937. [CrossRef] [PubMed]
35. Sathasivam, K.; Garip, I.; Saeed, S.H.; Yais, Y.; Alanssari, A.I.; Hussein, A.A.; Hammoode, J.A.; Lafta, A.M. A Novel MPPT Method Based on PSO and ABC Algorithms for Solar Cell. *Electr. Power Compon. Syst.* **2024**, *52*, 653–664. [CrossRef]
36. Hadi, N.; Jalal, B. Investigation of river water pollution using Muskingum method and particle swarm optimization (PSO) algorithm. *Appl. Water Sci.* **2024**, *14*, 68.
37. Shaikh, M.S.; Raj, S.; Babu, R.; Kumar, S.; Sagrolikar, K. A hybrid moth–flame algorithm with particle swarm optimization with application in power transmission and distribution. *Decis. Anal. J.* **2023**, *6*, 100182. [CrossRef]
38. Makhija, D.; Sudhakar, C.; Reddy, P.B.; Kumari, V. Workflow Scheduling in Cloud Computing Environment by Combining Particle Swarm Optimization and Grey Wolf Optimization. *Comput. Sci. Eng. Int. J.* **2022**, *12*, 1–10. [CrossRef]
39. Adekilekun, M.T.; Abiola, G.A.; Olajide, M.O. Hybrid Optimization Technique for Solving Combined Economic Emission Dispatch Problem of Power Systems. *Turk. J. Electr. Power Energy Syst.* **2022**, *2*, 158–167.
40. Osei-Kwakye, J.; Han, F.; Amponsah, A.A.; Ling, Q.; Abeo, T.A. A hybrid optimization method by incorporating adaptive response strategy for Feedforward neural network. *Connect. Sci.* **2022**, *34*, 578–607. [CrossRef]
41. Wang, N.; Wang, J.S.; Zhu, L.F.; Wang, H.Y.; Wang, G. A novel dynamic clustering method by integrating marine predators algorithm and particle swarm optimization algorithm. *IEEE Access* **2020**, *9*, 3557–3569. [CrossRef]
42. Samantaray, S.; Sahoo, P.; Sahoo, A.; Satapathy, D.P. Flood discharge prediction using improved ANFIS model combined with hybrid particle swarm optimisation and slime mould algorithm. *Environ. Sci. Pollut. Res.* **2023**, *30*, 83845–83872. [CrossRef]
43. Wang, D.; Liu, L.; Ben, Y.; Dai, P.; Wang, J. Seabed Terrain-Aided Navigation Algorithm Based on Combining Artificial Bee Colony and Particle Swarm Optimization. *Appl. Sci.* **2023**, *13*, 1166. [CrossRef]
44. Agushaka, J.O.; Ezugwu, A.E.; Abualigah, L. Gazelle optimization algorithm: A novel nature-inspired metaheuristic optimizer. *Neural Comput. Appl.* **2023**, *35*, 4099–4131. [CrossRef]
45. Lu, W.; Shi, C.; Fu, H.; Xu, Y. A Power Transformer Fault Diagnosis Method Based on Improved Sand Cat Swarm Optimization Algorithm and Bidirectional Gated Recurrent Unit. *Electronics* **2023**, *12*, 672. [CrossRef]
46. Nan, A.; Liyong, B. Particle Swarm Algorithm Based on Homogenized Logistic Mapping and Its Application in Antenna Parameter Optimization. *Int. J. Inf. Commun. Sci.* **2022**, *7*, 1–6.

47. Yang, D.D.; Mei, M.; Zhu, Y.J.; He, X.; Xu, Y.; Wu, W. Coverage Optimization of WSNs Based on Enhanced Multi-Objective Salp Swarm Algorithm. *Appl. Sci.* **2023**, *13*, 11252. [CrossRef]
48. Wei, X.; Zhang, Y.; Zhao, Y. Evacuation path planning based on the hybrid improved sparrow search optimization algorithm. *Fire* **2023**, *6*, 380. [CrossRef]
49. Zheng, X.; Nie, B.; Chen, J.; Du, Y.; Zhang, Y.; Jin, H. An improved particle swarm optimization combined with double-chaos search. *Math. Biosci. Eng.* **2023**, *20*, 15737–15764. [CrossRef]
50. Ozcan, E.; Mohan, C.K. Particle swarm optimization: Surfing the waves. In Proceedings of the 1999 Congress on Evolutionary Computation-CEC99 (Cat. No. 99TH8406), Washington, DC, USA, 6–9 July 1999; IEEE: Piscataway, NJ, USA, 1999; Volume 3, pp. 1939–1944.
51. Mirjalili, S.; Mirjalili, S.M.; Lewis, A. Grey wolf optimizer. *Adv. Eng. Softw.* **2014**, *69*, 46–61. [CrossRef]
52. Mirjalili, S. SCA: A sine cosine algorithm for solving optimization problems. *Knowl. -Based Syst.* **2016**, *96*, 120–133. [CrossRef]
53. Abualigah, L.; Diabat, A.; Mirjalili, S.; Abd Elaziz, M.; Gandomi, A.H. The arithmetic optimization algorithm. *Comput. Methods Appl. Mech. Eng.* **2021**, *376*, 113609. [CrossRef]
54. Storn, R.; Price, K. Differential evolution–a simple and efficient heuristic for global optimization over continuous spaces. *J. Glob. Optim.* **1997**, *11*, 341–359. [CrossRef]
55. Khishe, M.; Mosavi, M.R. Chimp optimization algorithm. *Expert Syst. Appl.* **2020**, *149*, 113338. [CrossRef]
56. Simon, D. Biogeography-based optimization. *IEEE Trans. Evol. Comput.* **2008**, *12*, 702–713. [CrossRef]
57. Chopra, N.; Ansari, M.M. Golden jackal optimization: A novel nature-inspired optimizer for engineering applications. *Expert Syst. Appl.* **2022**, *198*, 116924. [CrossRef]

Disclaimer/Publisher's Note: The statements, opinions and data contained in all publications are solely those of the individual author(s) and contributor(s) and not of MDPI and/or the editor(s). MDPI and/or the editor(s) disclaim responsibility for any injury to people or property resulting from any ideas, methods, instructions or products referred to in the content.